PROD. TYPE: COM
ED: Jolly
ARTICLE IN PRESS

PERGAMON

International Journal of Hydrogen Energy ▮▮▮ (▮▮▮▮) ▮▮▮–▮▮▮

International Journal of HYDROGEN ENERGY

www.elsevier.com/locate/ijhydene

Vibrational spectral emission of fractional-principal-quantum-energy-level hydrogen molecular ion

Randell L. Mills *, Paresh Ray

BlackLight Power, Inc., 493 Old Trenton Road, Cranbury, NJ 08512, USA

Abstract

From a solution of a Schrödinger-type wave equation with a nonradiative boundary condition based on Maxwell's equations, Mills solves the hydrogen atom, the hydrogen molecular ion, the hydrogen molecule, and predicts corresponding species having fractional principal quantum numbers. Atomic hydrogen may undergo a catalytic reaction with certain atomized elements and ions which singly or multiply ionize at integer multiples of the potential energy of atomic hydrogen, $m27.2$ eV wherein m is an integer. The reaction involves a nonradiative energy transfer to form a hydrogen atom $H(1/p)$ that is lower in energy than unreacted atomic hydrogen that corresponds to a fractional principal quantum number ($n = 1/p = 1/\text{integer}$ replaces the well known parameter n = integer in the Rydberg equation for hydrogen excited states). One such atomic catalytic system involves argon ions. The reaction Ar^+ to Ar^{2+} has a net enthalpy of reaction of 27.63 eV, which is equivalent to $m = 1$. Thus, it may serve as a catalyst to form $H(\frac{1}{2})$. Also, the second ionization energy of helium is 54.4 eV; thus, the ionization reaction of He^+ to He^{2+} has a net enthalpy of reaction of 54.4 eV which is equivalent to 2×27.2 eV. The products of the catalysis reaction $H(\frac{1}{3})$ may further serve as a catalyst to form $H(\frac{1}{4})$ and $H(\frac{1}{2})$. $H(1/p)$ may react with a proton to form an excited state molecular ion $H_2^*(1/p)^+$ that has a bond energy and vibrational levels that are p^2 times those of the molecular ion comprising uncatalyzed atomic hydrogen where p is an integer. Thus, the excited state spectrum of $H_2^*[n = \frac{1}{4}; n^* = 2]^+$ was predicted to comprise rotationally broadened vibrational transitions at 1.185 eV increments to the dissociation limit of $H_2[n = \frac{1}{4}]^+$, $E_D = 42.88$ eV (28.92 nm). Extreme ultraviolet spectroscopy was recorded on microwave discharges of argon or helium with 10% hydrogen in the range 10–65 nm. Novel emission lines assigned to vibrational transitions of $H_2^*[n = \frac{1}{4}; n^* = 2]^+$ were observed in this range with energies of $v1.185$ eV, $v = 17$–38 that terminated at about 28.9 nm. In addition, fractional molecular hydrogen rotational transitions were assigned to previously unidentified lines in the Solar coronal spectrum that matched theoretical predictions to five figures. © 2001 Published by Elsevier Science Ltd on behalf of the International Association for Hydrogen Energy.

1. Introduction

1.1. Background

J.J. Balmer showed in 1885 that the frequencies for some of the lines observed in the emission spectrum of atomic hydrogen could be expressed with a completely empirical relationship. This approach was later extended by J.R. Rydberg, who showed that all of the spectral lines of atomic hydrogen were given by the equation:

$$\bar{v} = R\left(\frac{1}{n_f^2} - \frac{1}{n_i^2}\right), \quad (1)$$

where $R = 109,677\ \text{cm}^{-1}$, $n_f = 1, 2, 3, \ldots$, $n_i = 2, 3, 4, \ldots$, and $n_i > n_f$.

Niels Bohr, in 1913, developed a theory for atomic hydrogen that gave energy levels in agreement with Rydberg's equation. An identical equation, based on a totally

* Corresponding author. Tel.: +1-609-490-1090; fax: +1-609-490-1066.
E-mail address: rmills@blacklightpower.com (R.L. Mills).

0360-3199/01/$ 20.00 © 2001 Published by Elsevier Science Ltd on behalf of the International Association for Hydrogen Energy.
PII: S0360-3199(01)00145-8

different theory for the hydrogen atom, was developed by E. Schrödinger, and independently by W. Heisenberg, in 1926

$$E_n = -\frac{e^2}{n^2 8\pi\varepsilon_0 a_H} = -\frac{13.598\ \text{eV}}{n^2}, \quad n = 1, 2, 3, \ldots, \tag{2a,b}$$

where a_H is the Bohr radius for the hydrogen atom (52.947 pm), e is the magnitude of the charge of the electron, and ε_0 is the vacuum permittivity. Based on the solution of a Schrödinger-type wave equation with a nonradiative boundary condition based on Maxwell's equations, Mills [1–27] predicts that atomic hydrogen may undergo a catalytic reaction with certain atomized elements or certain gaseous ions which singly or multiply ionize at integer multiples of the potential energy of atomic hydrogen, 27.2 eV. The reaction involves a nonradiative energy transfer to form a hydrogen atom that is lower in energy than unreacted atomic hydrogen that corresponds to a fractional principal quantum number where Eq. (2b), should be replaced by

$$n = 1, 2, 3, \ldots, \quad \text{and} \quad n = \tfrac{1}{2}, \tfrac{1}{3}, \tfrac{1}{4}, \ldots . \tag{2c}$$

A number of independent experimental observations lead to the conclusion that atomic hydrogen can exist in fractional quantum states that are at lower energies than the traditional "ground" ($n = 1$) state.

1.2. Experimental data of lower-energy hydrogen

Observation of intense extreme ultraviolet (EUV) emission at low temperatures (e.g. $\approx 10^3$ K) from atomic hydrogen and certain atomized elements or certain gaseous ions [8,9,12–14,16–18] has been reported previously. The only pure elements that were observed to emit EUV were those wherein the ionization of t electrons from an atom to a continuum energy level is such that the sum of the ionization energies of the t electrons is approximately $m27.2$ eV where t and m are each an integer. Potassium, cesium, and strontium atoms and Rb^+ ion ionize at integer multiples of the potential energy of atomic hydrogen and caused emission. Whereas, the chemically similar atoms, sodium, magnesium and barium, do not ionize at integer multiples of the potential energy of atomic hydrogen and caused no emission.

Additional prior related studies that support the possibility of a novel reaction of atomic hydrogen which produces a chemically generated or assisted plasma and produces novel hydride compounds include EUV spectroscopy [7–18], characteristic emission from catalysis and the hydride ion product [8,9], lower-energy hydrogen emission [7–9], plasma formation [8,9,12–14,16–18], Balmer α line broadening [10], anomalous plasma afterglow duration [16,17], power generation [10,11,18], and analysis of chemical compounds [19–25]. Exemplary related studies include:

(1) The observation of novel EUV emission lines from microwave and glow discharges of helium with 2% hydrogen with energies of $q13.6$ eV where $q = 1, 2, 3, 4, 6, 7, 8, 9$, or 11 or these lines inelastically scattered by helium atoms in the excitation of $He(1s^2)$ to $He(1s^1 2p^1)$ that were identified as hydrogen transitions to electronic energy levels below the "ground" state corresponding to fractional quantum numbers [7],

(2) the identification of transitions of atomic hydrogen to lower energy levels corresponding to lower energy hydrogen atoms in the extreme ultraviolet emission spectrum from interstellar medium and the Sun [1,5,7],

(3) the EUV spectroscopic observation of lines by the Institut für Niedertemperatur-Plasmaphysik e.V. that could be assigned to transitions of atomic hydrogen to lower energy levels corresponding to fractional principal quantum numbers and the emission from the excitation of the corresponding hydride ions [15],

(4) the recent analysis of mobility and spectroscopy data of individual electrons in liquid helium which shows direct experimental confirmation that electrons may have fractional principal quantum energy levels [6],

(5) the observation of continuum state emission of Cs^{2+} and Ar^{2+} at 53.3 and 45.6 nm, respectively, with the absence of the other corresponding Rydberg series of lines from these species which confirmed the resonant nonradiative energy transfer of 27.2 eV from atomic hydrogen to the catalysts atomic cesium or Ar^+ [9],

(6) the spectroscopic observation of the predicted hydride ion $H^-(\frac{1}{4})$ of hydrogen catalysis by either cesium atom or Ar^+ catalyst at 407 nm corresponding to its predicted binding energy of 3.05 eV [9],

(7) the observation of characteristic emission from K^{3+} which confirmed the resonant nonradiative energy transfer of 3.27.2 eV from atomic hydrogen to atomic potassium [8],

(8) the spectroscopic observation of the predicted $H^-(\frac{1}{4})$ hydride ion of hydrogen catalysis by potassium catalyst at 110 nm corresponding to its predicted binding energy of 11.2 eV [8],

(9) the observation by the Institut für Niedertemperatur-Plasmaphysik e.V. of an anomalous plasma and plasma afterglow duration formed with hydrogen–potassium mixtures [16],

(10) the observation of anomalous afterglow durations of plasmas formed by catalysts providing a net enthalpy of reaction within thermal energies of $m27.28$ eV [16,17],

(11) the observation of Lyman series in the EUV that represents an energy release 10 times hydrogen combustion which is greater than that of any possible known chemical reaction [7,18],

(12) the observation of line emission by the Institut für Niedertemperatur-Plasmaphysik e.V. with a 4° grazing incidence EUV spectrometer that was 100 times more energetic than the combustion of hydrogen [15],

(13) the observation of anomalous plasmas formed with strontium and argon catalysts at 1% of the theoretical

or prior known voltage requirement with a light output for power input up to 8600 times that of the control standard light source [12,13,18],

(14) the observation that the optically measured output power of gas cells for power supplied to the glow discharge increased by over two orders of magnitude depending on the presence of less than 1% partial pressure of certain catalysts in hydrogen gas or argon–hydrogen gas mixtures, and an excess thermal balance of 42 W was measured for the 97% argon and 3% hydrogen mixture versus argon plasma alone [11],

(15) the observation that plasmas of the catalyst–hydrogen mixtures of strontium–hydrogen, helium–hydrogen, argon–hydrogen, strontium–helium–hydrogen, and strontium–argon–hydrogen showed significant Balmer α line broadening corresponding to an average hydrogen atom temperature of 25–45 eV; whereas, plasmas of the noncatalyst–hydrogen mixtures of pure hydrogen, krypton–hydrogen, xenon–hydrogen, and magnesium–hydrogen showed no excessive broadening corresponding to an average hydrogen atom temperature of ≈ 3 eV [10],

(16) the observation that the power emitted for power supplied to a hydrogen glow discharge plasmas increased by 35–184 W depending on the presence of catalysts helium or argon and less than 1% partial pressure of strontium metal in noble gas–hydrogen mixtures; whereas, the chemically similar noncatalyst krypton had no effect on the power balance [10],

(17) the differential scanning calorimetry (DSC) measurement of minimum heats of formation of KHI by the catalytic reaction of potassium with atomic hydrogen and KI that were over −2000 kJ/mol H_2 compared to the enthalpy of combustion of hydrogen of −241.8 kJ/mol H_2 [25],

(18) the isolation of novel hydrogen compounds as products of the reaction of atomic hydrogen with atoms and ions which formed an anomalous plasma as reported in the EUV studies [19–25],

(19) the identification of novel hydride compounds by (i) time of flight secondary ion mass spectroscopy which showed a dominant hydride ion in the negative ion spectrum, (ii) X-ray photoelectron spectroscopy which showed novel hydride peaks and significant shifts of the core levels of the primary elements bound to the novel hydride ions, (iii) ^{1}H nuclear magnetic resonance spectroscopy (NMR) which showed extraordinary upfield chemical shifts compared to the NMR of the corresponding ordinary hydrides, and (iv) thermal decomposition with analysis by gas chromatography, and mass spectroscopy which identified the compounds as hydrides [19–25],

(20) the NMR identification of novel hydride compounds MH^*X wherein M is the metal, X, is a halide, and H^* comprises a novel high binding energy hydride ion identified by a large distinct upfield resonance [19,20,23],

(21) the replication of the NMR results of the identification of novel hydride compounds by large distinct upfield resonances at Spectral Data Services, University of Massachusetts Amherst, University of Delaware, Grace Davison, and National Research Council of Canada [19], and

(22) the NMR identification of novel hydride compounds MH^* and MH_2^* wherein M is the metal and H^* comprises a novel high binding energy hydride ion identified by a large distinct upfield resonance that proves the hydride ion is different from the hydride ion of the corresponding known compound of the same composition [19].

1.3. Mechanism of the formation of lower-energy atomic hydrogen

The mechanism of the EUV emission, the formation of novel hydrides, and the observation of certain EUV lines from interstellar medium and the Sun cannot be explained by the conventional energy levels of hydrogen, but it is predicted by a solution of the Schrödinger equation with a nonradiative boundary constraint put forward by Mills [1]. Mills predicts that certain atoms or ions serve as catalysts to release energy from hydrogen to produce an increased binding energy hydrogen atom called a *hydrino atom* having a binding energy given by Eq. (2a) where

$$n = \frac{1}{2}, \frac{1}{3}, \frac{1}{4}, \ldots, \frac{1}{p} \tag{3}$$

and p is an integer greater than 1, designated as $H[a_H/p]$ where a_H is the radius of the hydrogen atom. Hydrinos are predicted to form by reacting an ordinary hydrogen atom with a catalyst having a net enthalpy of reaction of about

$$m27.21 \text{ eV}, \tag{4}$$

where m is an integer. This catalysis releases energy from the hydrogen atom with a commensurate decrease in size of the hydrogen atom, $r_n = na_H$. For example, the catalysis of $H(n = 1)$ to $H(n = \frac{1}{2})$ releases 40.8 eV, and the hydrogen radius decreases from a_H to $\frac{1}{2}a_H$.

The excited energy states of atomic hydrogen are also given by Eq. (2a) except with Eq. (2b). The $n = 1$ state is the "ground" state for "pure" photon transitions (the $n = 1$ state can absorb a photon and go to an excited electronic state, but it cannot release a photon and go to a lower-energy electronic state). However, an electron transition from the ground state to a lower-energy state is possible by a nonradiative energy transfer such as multipole coupling or a resonant collision mechanism. These lower-energy states have fractional quantum numbers, $n = 1/\text{integer}$.

Processes that occur without photons and that require collisions are common. For example, the exothermic chemical reaction of H + H to form H_2 does not occur with the

emission of a photon. Rather, the reaction requires a collision with a third body, M, to remove the bond energy — $H + H + M \rightarrow H_2 + M^*$ [28]. The third body distributes the energy from the exothermic reaction, and the end result is the H_2 molecule and an increase in the temperature of the system. Some commercial phosphors are based on nonradiative energy transfer involving multipole coupling. For example, the strong absorption strength of Sb^{3+} ions along with the efficient nonradiative transfer of excitation from Sb^{3+} to Mn^{2+}, are responsible for the strong manganese luminescence from phosphors containing these ions [29]. Similarly, the $n = 1$ state of hydrogen and the $n = 1/\text{integer}$ states of hydrogen are nonradiative, but a transition between two nonradiative states is possible via a nonradiative energy transfer, say $n = 1 - \frac{1}{2}$. In these cases, during the transition the electron couples to another electron transition, electron transfer reaction, or inelastic scattering reaction which can absorb the exact amount of energy that must be removed from the hydrogen atom to cause the transition. Thus, a catalyst provides a net positive enthalpy of reaction of $m27.21$ eV (i.e. it absorbs $m27.21$ eV where m is an integer). Certain atoms or ions serve as catalysts which resonantly accept energy from hydrogen atoms and release the energy to the surroundings to effect electronic transitions to fractional quantum energy levels. Recent analysis of mobility and spectroscopy data of individual electrons in liquid helium show direct experimental evidence that electrons may have fractional principal quantum energy levels [6].

The catalysis of hydrogen involves the nonradiative transfer of energy from atomic hydrogen to a catalyst which may then release the transferred energy by radiative and nonradiative mechanisms. As a consequence of the nonradiative energy transfer, the hydrogen atom becomes unstable and emits further energy until it achieves a lower-energy nonradiative state having a principal energy level given by Eqs. (2a) and (3).

1.4. Catalysts

According to Mills [1], a catalytic system is provided by the ionization of t electrons from an atom or ion to a continuum energy level such that the sum of the ionization energies of the t electrons is approximately $m27.2$ eV where m is an integer.

1.4.1. Argon ions

Argon ions can provide a net enthalpy of a multiple of that of the potential energy of the hydrogen atom. The second ionization energy of argon is 27.63 eV. The reaction Ar^+ to Ar^{2+} has a net enthalpy of reaction of 27.63 eV, which is equivalent to $m = 1$ in Eq. (4)

$$27.63\text{ eV} + Ar^+ + H\left[\frac{a_H}{p}\right] \rightarrow Ar^{2+} + e^- + H\left[\frac{a_H}{(p+1)}\right] + [(p+1)^2 - p^2]13.6\text{ eV}, \quad (5)$$

$$Ar^{2+} + e^- \rightarrow Ar^+ + 27.63\text{ eV}. \quad (6)$$

And, the overall reaction is

$$H\left[\frac{a_H}{p}\right] \rightarrow H\left[\frac{a_H}{(p+1)}\right] + [(p+1)^2 - p^2]13.6\text{ eV}. \quad (7)$$

1.4.2. Helium ion

Helium ion (He^+) is also such a catalyst because the second ionization energy of helium is 54.417 eV, which is equivalent to $m = 2$ in Eq. (4). In this case, the catalysis reaction is

$$54.417\text{ eV} + He^+ + H[a_H] \rightarrow He^{2+} + e^- + H\left[\frac{a_H}{3}\right] + 108.8\text{ eV}, \quad (8)$$

$$He^{2+} + e^- \rightarrow He^+ + 54.417\text{ eV}. \quad (9)$$

And, the overall reaction is

$$H[a_H] \rightarrow H\left[\frac{a_H}{3}\right] + 54.4\text{ eV} + 54.4\text{ eV}. \quad (10)$$

The energy given off during catalysis is much greater than the energy lost to the catalyst. The energy released is large as compared to conventional chemical reactions. For example, when hydrogen and oxygen gases undergo combustion to form water

$$H_2(g) + \tfrac{1}{2}O_2(g) \rightarrow H_2O(l) \quad (11)$$

the known enthalpy of formation of water is $\Delta H_f = -286$ kJ/mol or 1.48 eV per hydrogen atom. By contrast, each ($n = 1$) ordinary hydrogen atom undergoing catalysis releases a net of 40.8 eV. Moreover, further catalytic transitions may occur: $n = \frac{1}{2} \rightarrow \frac{1}{3}$, $\frac{1}{3} \rightarrow \frac{1}{4}$, $\frac{1}{4} \rightarrow \frac{1}{5}$, and so on. Once catalysis begins, hydrinos autocatalyze further in a process called *disproportionation*. This mechanism is similar to that of an inorganic ion catalysis. But, hydrino catalysis should have a higher reaction rate than that of the inorganic ion catalyst due to the better match of the enthalpy to $m27.2$ eV.

1.4.3. Hydrino catalysts

In a process called *disproportionation*, lower-energy hydrogen atoms, *hydrinos*, can act as catalysts because each of the metastable excitation, resonance excitation, and ionization energy of a hydrino atom is $m27.2$ eV (Eq. (4)). The transition reaction mechanism of a first hydrino atom affected by a second hydrino atom involves the resonant coupling between the atoms of m degenerate multipoles each having 27.21 eV of potential energy [1]. The energy transfer of $m27.2$ eV from the first hydrino atom to the second hydrino atom causes the central field of the first atom to increase by m and its electron to drop m levels lower from a radius of a_H/p to a radius of $a_H/(p + m)$. The second interacting

lower-energy hydrogen is either excited to a metastable state, excited to a resonance state, or ionized by the resonant energy transfer. The resonant transfer may occur in multiple stages. For example, a nonradiative transfer by multipole coupling may occur wherein the central field of the first increases by m, then the electron of the first drops m levels lower from a radius of a_H/p to a radius of $a_H/(p+m)$ with further resonant energy transfer. The energy transferred by multipole coupling may occur by a mechanism that is analogous to photon absorption involving an excitation to a virtual level. Or, the energy transferred by multipole coupling during the electron transition of the first hydrino atom may occur by a mechanism that is analogous to two photon absorption involving a first excitation to a virtual level and a second excitation to a resonant or continuum level [30–32]. The transition energy greater than the energy transferred to the second hydrino atom may appear as a photon in a vacuum medium.

The transition of $H[a_H/p]$ to $H[a_H/(p+m)]$ induced by a multipole resonance transfer of $m27.21$ eV (Eq. (4)) and a transfer of $[(p')^2-(p'-m')^2]13.6$ eV $-m27.2$ eV with a resonance state of $H[a_H/(p'-m')]$ excited in $H[a_H/p']$ is represented by

$$H\left[\frac{a_H}{p'}\right]+H\left[\frac{a_H}{p}\right]\rightarrow H\left[\frac{a_H}{p'-m'}\right]+H\left[\frac{a_H}{p+m}\right]$$
$$+[((p+m)^2-p^2)-(p'^2-(p'-m')^2)]13.6\text{ eV}, \quad (12)$$

where p, p', m, and m' are integers.

Hydrinos may be ionized during a disproportionation reaction by the resonant energy transfer. A hydrino atom with the initial lower-energy state quantum number p and radius a_H/p may undergo a transition to the state with lower-energy state quantum number $(p+m)$ and radius $a_H/(p+m)$ by reaction with a hydrino atom with the initial lower-energy state quantum number m', initial radius a_H/m', and final radius a_H that provides a net enthalpy of $m27.2$ eV (Eq. (4)). Thus, reaction of hydrogen-type atoms $H[a_H/p]$, with the hydrogen-type atom, $H[a_H/m']$, that is ionized by the resonant energy transfer to cause a transition reaction is represented by

$$m27.21\text{ eV}+H\left[\frac{a_H}{m'}\right]+H\left[\frac{a_H}{p}\right]\rightarrow H^+$$
$$+e^-+H\left[\frac{a_H}{(p+m)}\right]+[(p+m)^2-p^2$$
$$-(m'^2-2m)]13.6\text{ eV}, \quad (13)$$

$$H^++e^-\rightarrow H\left[\frac{a_H}{1}\right]+13.6\text{ eV}. \quad (14)$$

And, the overall reaction is

$$H\left[\frac{a_H}{m'}\right]+H\left[\frac{a_H}{p}\right]$$
$$\rightarrow H\left[\frac{a_H}{1}\right]+H\left[\frac{a_H}{(p+m)}\right]+[2pm+m^2-m'^2]$$
$$13.6\text{ eV}+13.6\text{ eV}. \quad (15)$$

Helium ion catalyzes $H[a_H]$ to $H[a_H/3]$ as shown in Eqs. (8)–(10). Disproportionation reaction may then proceed to give:

$$H\left[\frac{a_H}{3}\right]+H\left[\frac{a_H}{3}\right]\rightarrow H\left[\frac{a_H}{4}\right]+H\left[\frac{a_H}{2}\right]+27.2\text{ eV} \quad (16)$$

1.5. The nature of the chemical bonds of the hydrogen molecular ion, the hydrogen molecule, and hydrogen molecular ions and molecules having fractional principal quantum numbers

From the application of the nonradiative boundary condition, the instability of excited states as well as the stability of the "ground" state arise naturally in the Mills theory [1] described in Appendix B. In addition to the known states of hydrogen (Eqs. (2a) and (2b)), the theory predicts the existence of a previously unknown form of matter: hydrogen atoms and molecules having electrons of lower energy than the conventional "ground" state, called *hydrinos* and *dihydrino* — the diatomic hydrino molecule, respectively, where each energy level corresponds to a fractional quantum number.

Two hydrogen atoms react to form a diatomic molecule, the hydrogen molecule

$$2H[a_H]\rightarrow H_2[2c'=\sqrt{2}a_0], \quad (17)$$

where $2c'$ is the internuclear distance. Also, two hydrino atoms react to form a diatomic molecule, a dihydrino molecule

$$2H\left[\frac{a_H}{p}\right]\rightarrow H_2\left[2c'=\frac{\sqrt{2}a_0}{p}\right], \quad (18)$$

where p is an integer. And, a hydrino atom can react with a proton to form a dihydrino molecular ion that further reacts with an electron to form a dihydrino molecule

$$H\left[\frac{a_H}{p}\right]+H^++e^-\rightarrow H_2\left[2c'=\frac{\sqrt{2}a_0}{p}\right]. \quad (19)$$

The hydrogen-type molecular ion and molecular charge and current density functions, bond distance, and energies are solved in Appendix B from the Laplacian in ellipsoidal

coordinates with the constraint of nonradiation

$$(\eta-\zeta)R_\xi\frac{\partial}{\partial\xi}\left(R_\xi\frac{\partial\phi}{\delta\xi}\right)+(\zeta-\xi)R_\eta\frac{\partial}{\partial\eta}\left(R_\eta\frac{\partial\phi}{\partial\eta}\right)$$

$$+(\xi-\eta)R_\zeta\frac{\partial}{\partial\zeta}\left(R_\zeta\frac{\partial\phi}{\partial\zeta}\right)=0. \quad (20)$$

In the case that a hydrino atom reacts with a proton to form a dihydrino molecular ion,

$$H\left[\frac{a_H}{p}\right]+H^+\rightarrow H_2\left[2c'=\frac{2a_0}{p}\right]^+ \quad (21)$$

a designation for this reaction in terms of quantum numbers is

$$H[n=1/p]+H^+\rightarrow H_2[n=1/p]^+. \quad (22)$$

The energy released is

$$E_D=E\left(H\left[\frac{a_H}{p}\right]\right)-E_T$$

$$=-p^2 13.6+p^2 16.28\,eV=p^2 2.68\,eV, \quad (23)$$

where E_T is given by Eq. (B.77). The reaction of a hydrino atom with a proton may involve an excited electronic state and a series of corresponding vibrational and rotational states. In the reaction designated

$$H\left[\frac{a_H}{2}\right]+H^+\rightarrow H_2^*\left[2c'=\frac{a_0}{4};n^*=2\right]^+ \quad (24)$$

the hydrino $H[n=\frac{1}{2}]$ may react with a proton to form the first excited electronic state of the molecular ion $H_2[n=\frac{1}{4}]^+$ wherein the central field in elliptic coordinates in one half that of ground state (nonradiative state) of $H_2[n=\frac{1}{4}]^+$. This state is analogous to the $n=2$ state of atomic hydrogen and is designated as $H_2^*[n=\frac{1}{4};n^*=2]^+$, except that electronic relaxation may involve a radiationless process with a radiative component involving the oscillating and rotating nuclei which undergoes transition to the ground state of $H_2[n=\frac{1}{4}]^+$. The nonradiative energy transfer corresponding to $H[n=\frac{1}{2}]\rightarrow H[n=\frac{1}{4}]$ may occur from the highest vibrational state (bond-continuum state) of $H_2[n=\frac{1}{2}]^+$. The bond energy of $H_2[n=1/p]^+$ is given by Eq. (B.78). Thus, the bond energy of $H_2[n=\frac{1}{4}]^+$ is

$$E_D=p^2 2.68\,eV=4^2 2.68\,eV=42.88\,eV(28.92\,nm), \quad (25)$$

where $p=4$, and the bond energy of $H_2[n=\frac{1}{2}]^+$ is

$$E_D=p^2 2.68\,eV=2^2 2.68\,eV=10.72\,eV(115.70\,nm), \quad (25)$$

where $p=2$. Due to the Franck–Condon principle, the vibrational and rotational energies of $H_2^*[n=\frac{1}{4};n^*=2]^+$ are equivalent to those of $H_2[n=\frac{1}{2}]^+$ given by Eq. (B.122) and Eq. (B.255), respectively,

$$E_{vib}=(v_f-v_i)p^2 0.2962\,eV=(v_f-v_i)1.185\,eV, \quad (26)$$

$$\lambda=\frac{169}{p^2[J+1]}\,\mu m=\frac{42}{[J+1]}\,\mu m\quad(J+1\rightarrow J), \quad (27)$$

where $p=2$. Thus, the emission spectrum of $H_2^*[n=\frac{1}{4};n^*=2]^+$ is predicted to comprise vibrational peaks centered at 1.185 eV spacing slit by 42 μm spaced peaks due to rotational transitions terminating at about $E_D(H_2[n=\frac{1}{4}]^+)=42.88\,eV(28.92\,nm)$. Nonlinearity at highly excited vibrational levels with translational, vibrational, and rotational interactions are anticipated to broaden the terminal peaks.

1.6. EUV spectroscopy detects lower-energy hydrogen

It was previously reported that extreme ultraviolet spectroscopy was recorded on microwave and glow discharges of helium with 2% hydrogen wherein helium and the product hydrinos served as catalysts [7]. Novel emission lines were observed with energies of $q13.6\,eV$, where $q=1,2,3,4,6,7,8,9$, or 11 or these lines inelastically scattered by helium atoms wherein 21.2 eV was absorbed in the excitation of $He(1s^2)$ to $He(1s^1 2p^1)$. These lines were identified as hydrogen transitions to electronic energy levels below the "ground" state corresponding to fractional quantum numbers. In addition, a comparison was made between the plasma results and astrophysical data. Similar lower-energy-hydrogen transitions were found that matched the spectral lines of the extreme ultraviolet background of interstellar space and Solar lines.

Also, previously reported lines observed at the Institut für Niedertemperatur-Plasmaphysik e.V. by EUV spectroscopy could be assigned to transitions of atomic hydrogen to lower energy levels corresponding to hydrinos and the emission from the excitation of the corresponding hydride ions [15]. For example, the product of the catalysis of atomic hydrogen with potassium metal, $H[a_H/4]$ may serve as both a catalyst and a reactant to form $H[a_H/3]$ and $H[a_H/6]$. The transition of $H[a_H/4]$ to $H[a_H/6]$ induced by a multipole resonance transfer of 54.4 eV(2.27.2 eV) and a transfer of 40.8 eV with a resonance state of $H[a_H/3]$ excited in $H[a_H/4]$ is represented by

$$H\left[\frac{a_H}{4}\right]+H\left[\frac{a_H}{4}\right]\rightarrow H\left[\frac{a_H}{6}\right]+H\left[\frac{a_H}{3}\right]+176.8\,eV. \quad (28)$$

The predicted 176.8 eV(7.02 nm) photon is a close match with the observed 7.30 nm line. The energy of this line emission corresponds to an equivalent temperature of 1,000,000 °C and an energy over 100 times the energy of combustion of hydrogen.

Since the Sun and stars contain significant amounts of He^+ and atomic hydrogen, catalysis of atomic hydrogen by He^+ as given by Eqs. (8)–(10) may occur. Also, the simultaneous ionization of two hydrogen atoms may provide a net enthalpy given by Eq. (4) to catalyze hydrino formation. Once formed, hydrinos have binding energies given by Eqs. (2a) and (3); thus, they may serve as reactants which provide a net enthalpy of reaction given by Eq. (4). Lower-energy atomic hydrogen may react to form the corresponding dihydrino molecules. Characteristic emissions from the Sun may identify dihydrino molecules.

The detection of atomic hydrogen in fractional quantum energy levels below the traditional "ground" state — hydrinos — was previously reported [1,5,7] by the assignment of soft X-ray emissions from the interstellar medium, the Sun, and stellar flares, and by assignment of certain lines obtained by the far-infrared absolute spectrometer (FIRAS) on the Cosmic Background Explorer. The detection of a new molecular species — the diatomic hydrino molecule — was reported by the assignment of certain infrared line emissions from the Sun. The detection of a new hydride species — hydrino hydride ion — was reported by the assignment of certain soft X-ray, ultraviolet (UV), and visible emissions from the Sun. This has implications for several unresolved astrophysical problems such as the identity of dark matter and the Solar neutrino paradox [1,7].

From Eq. (26), the energy for the $v + 1 \rightarrow v$ vibrational transition is 1.185 eV. The increment of the McPherson 4° grazing incidence EUV spectrometer was 0.1 nm as described in Section 2. The corresponding energy in this spectral region is about 0.15 eV. The rotational levels given by Eq. (27) could not be resolved since the $J + 1 \rightarrow J$ corresponds to 0.03 eV. Thus, the excited state spectrum of $H_2^*[n = \frac{1}{4}; n^* = 2]^+$ was predicted to comprise rotationally broadened vibrational transitions centered on 1.185 eV increments. The series of vibrational transitions was predicted to terminate at about the dissociation limit of $H_2[n = \frac{1}{4}]^+$, $E_D = 42.88$ eV(28.92 nm) given by Eq. (25). We report that this spectrum was observed during microwave discharges of mixtures of argon or helium and 10% hydrogen. Solar astrophysical data was reviewed and emission lines from the corona were identified which matched dihydrino molecular rotational transitions to five figures.

2. Experimental

2.1. EUV spectroscopy

EUV spectroscopy was recorded on a microwave cell light source. Due to the extremely short wavelength of this radiation, "transparent" optics do not exist. Therefore, a windowless arrangement was used wherein the microwave cell was connected to the same vacuum vessel as the grating and detectors of the EUV spectrometer. Differential pumping permitted a high pressure in the cell as compared to that in the spectrometer. This was achieved by pumping on the cell outlet and pumping on the grating side of the collimator that served as a pinhole inlet to the optics. The spectrometer was continuously evacuated to 10^{-4}–10^{-6} Torr by a turbomolecular pump with the pressure read by a cold cathode pressure gauge. The EUV spectrometer was connected to the cell light source with a 1.5 mm × 5 mm collimator which provided a light path to the slits of the EUV spectrometer. The collimator also served as a flow constrictor of gas from the cell. The cell was operated under gas flow conditions while maintaining a constant gas pressure in the cell.

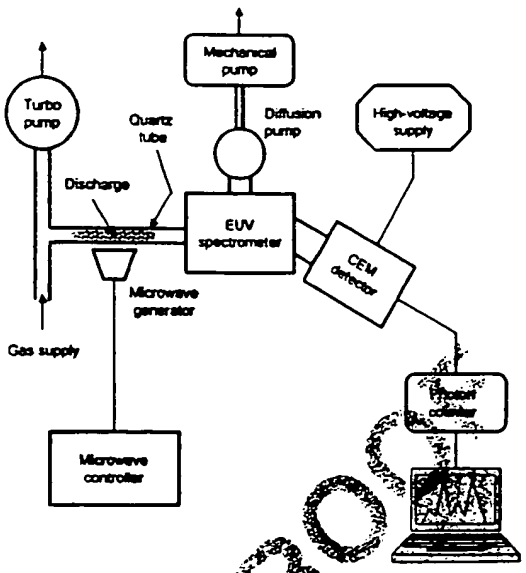

Fig. 1. The experimental setup comprising a microwave discharge gas cell light source and an EUV spectrometer which was differentially pumped.

EUV spectroscopy was recorded on argon–hydrogen ($\frac{90}{10}$%) and helium–hydrogen ($\frac{90}{10}$%) plasmas. The plasma source was a microwave plasma discharge cell. The microwave EUV spectra were recorded with a grazing incidence EUV spectrometer. Control plasmas of neon, krypton, xenon, hydrogen, argon, and helium alone and neon–hydrogen ($\frac{90}{10}$%), krypton–hydrogen ($\frac{90}{10}$%) and xenon–hydrogen ($\frac{90}{10}$%) were recorded.

The light emission from a microwave plasma was introduced to an EUV spectrometer for spectral measurement. The spectrometer was a McPherson 4° grazing incidence EUV spectrometer (Model 248/310G) equipped with a grating having 600 G/mm with a radius of curvature of ≈ 1 m. The angle of incidence was 87°. The wavelength region covered by the monochromator was 5–65 nm. The wavelength resolution was about 0.1 nm (FWHM) with an entrance and exit slit width of 300 μm. A channel electron multiplier (CEM) at 2400 V was used to detect the EUV light. The increment was 0.1 nm and the dwell time was 1 s.

2.2. Microwave emission spectra

The experimental setup comprising the microwave discharge gas cell light source and the EUV spectrometer which was differentially pumped is shown in Fig. 1. The extreme ultraviolet emission spectrum was obtained on plasmas of hydrogen alone, noble gases alone, or noble gas–hydrogen

mixtures ($\frac{90}{10}$%) with a microwave discharge system and an EUV spectrometer. Gas was flowed through a half-inch diameter quartz tube. The gas pressure inside the cell was maintained at about 300 mTorr under flow conditions where the flow of each gas was controlled by 0–20 sccm range mass flow controller (MKS 1179A21CS1BB) with a readout (MKS type 246). The flow rate for each gas tested alone was 11 sccm, and the flow rates for the neon, krypton, xenon, argon, or helium 90% with 10% hydrogen was 10 and 1 sccm, respectively. The pressure was measured with a 10 and 1000 Torr MKS Baratron absolute pressure gauge. The tube was fitted with an Opthos coaxial microwave cavity (Evenson cavity). The microwave generator was a Opthos model MPG-4M generator (frequency: 2450 MHz). The output power was set at 85 W. The EUV spectrometer was a McPherson 4° grazing incidence EUV spectrometer (Model 248/310G). (See EUV-Spectroscopy Section).

3. Results and discussion

3.1. EUV spectroscopy

The EUV emission spectra were recorded from microwave discharge plasmas of pure neon, krypton, xenon, hydrogen, argon, and helium, as well as 10% hydrogen with neon, krypton, xenon, argon, and helium over the wavelength range 20–60 nm. The short wavelength spectra of neon and neon–hydrogen ($\frac{90}{10}$%) were equivalent to the spectra reported previously [7]. Only known Ne II peaks were observed in this region. The EUV spectra of the control krypton and krypton–hydrogen ($\frac{90}{10}$%), xenon and xenon–hydrogen ($\frac{90}{10}$%), hydrogen, argon, and helium microwave discharge cell emission is shown in Figs. 2, 3, 4, 5, and 6,

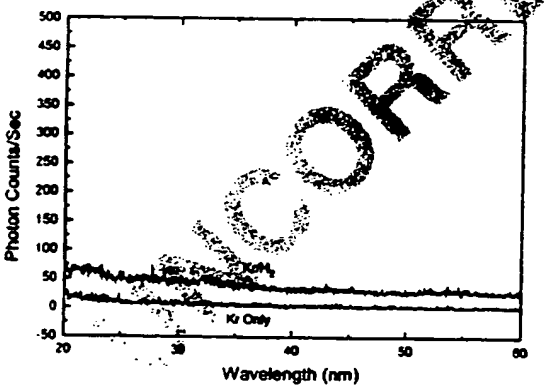

Fig. 2. The EUV spectra (20–60 nm) of the control krypton and krypton–hydrogen microwave discharge cell emission that were recorded with a 4° grazing incidence EUV spectrometer and a CEM. No emission was observed in this region with or without hydrogen.

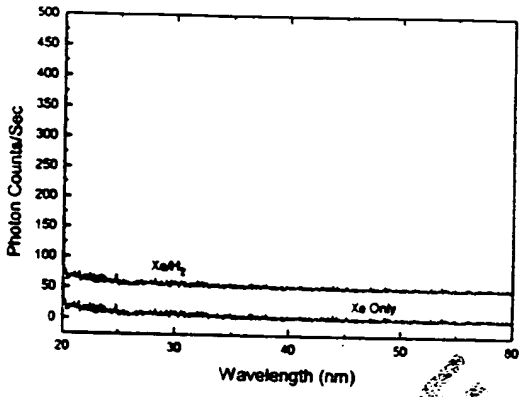

Fig. 3. The EUV spectra (20–60 nm) of the control xenon and xenon–hydrogen microwave discharge cell emission that were recorded with a 4° grazing incidence EUV spectrometer and a CEM. No emission was observed in this region with or without hydrogen.

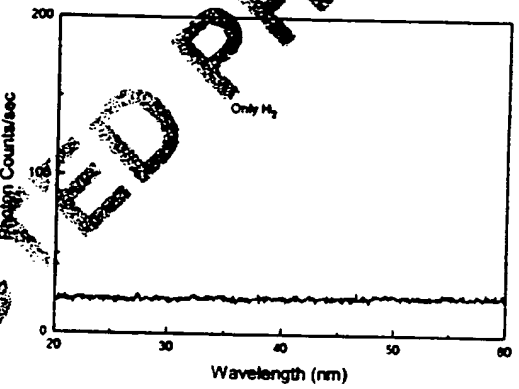

Fig. 4. The EUV spectrum (20–60 nm) of the control hydrogen microwave discharge cell emission that were recorded with a 4° grazing incidence EUV spectrometer and a CEM. No emission was observed in this region.

respectively. No spurious peaks or artifacts due to the grating or the spectrometer were observed. No changes in the emission spectra were observed by the addition of hydrogen to noncatalysts neon, krypton, or xenon.

The reaction Ar^+ to Ar^{2+} has a net enthalpy of reaction of 27.63 eV, which is equivalent to $m = 1$. The catalysis reaction involves a nonradiative energy transfer to form a hydrogen atom that is lower in energy than unreacted atomic hydrogen. The product hydrogen atom has an energy state that corresponds to a fractional principal quantum number. The lower-energy hydrogen atom is a highly reactive intermediate which further reacts to form a novel hydride ion. Emission was observed previously from a continuum state

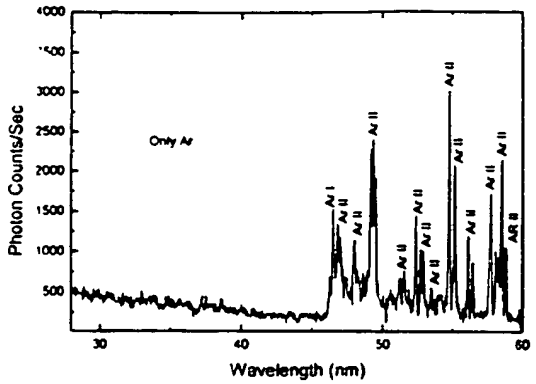

Fig. 5. The EUV spectrum (27–60 nm) of the control argon microwave discharge cell emission that was recorded with a 4° grazing incidence EUV spectrometer and a CEM. No emission was observed below 45 nm.

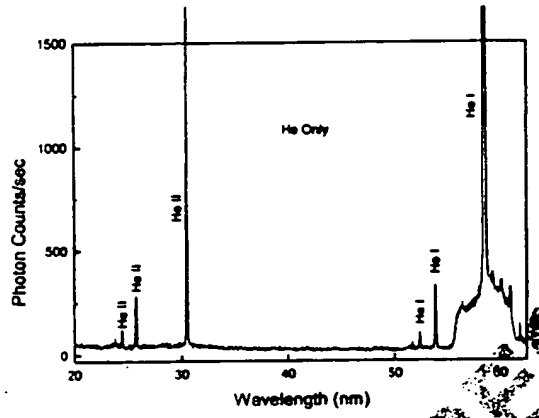

Fig. 6. The EUV spectrum (20–62 nm) of the control helium microwave discharge cell emission that was recorded with a 4° grazing incidence EUV spectrometer and a CEM. Only known line emission of He I and He II were observed.

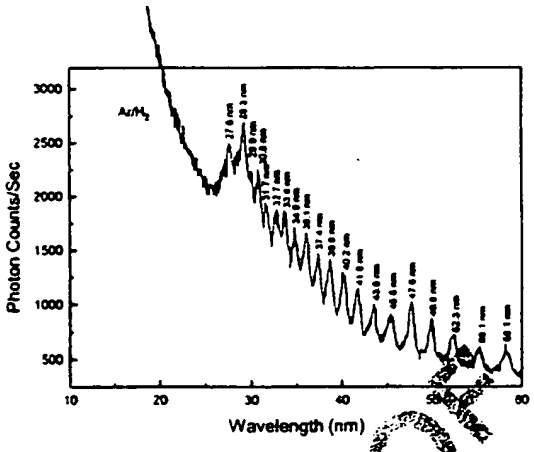

Fig. 7. The EUV spectrum (10–60 nm) of the argon–hydrogen mixture ($\frac{90}{10\%}$) microwave cell emission recorded with 0.1 nm increment of the McPherson 4° grazing incidence EUV spectrometer. A series of 0.5 eV wide Gaussian-shaped peaks were observed in the spectral region 27–60 nm that were assigned to the $v = 18$–38 vibrational transitions of $H_2^*[n = \frac{1}{4};\ n^* = 2]^+$ with energies $v1.185$ eV as given in Table 1. The intense continuum peak at about 28 nm that terminated the series was assigned to the dissociation energy of $H_2[n = \frac{1}{4}]^+$.

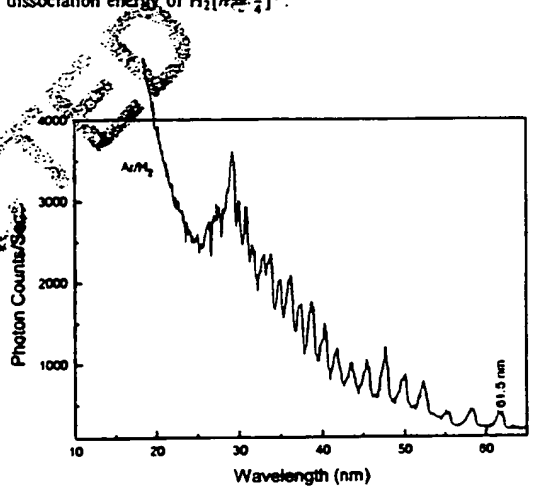

Fig. 8. The EUV spectrum (10–65 nm) of the argon–hydrogen mixture ($\frac{90}{10\%}$) microwave cell emission recorded with 0.1 nm increment of the McPherson 4° grazing incidence EUV spectrometer. With an increased spectral range compared to that of Fig. 7, an addition peak was observed at 61.5 nm that was assigned to the $v = 17$ vibrational transition of $H_2^*[n = \frac{1}{4};\ n^* = 2]^+$ with an energy $v1.185$ eV as given in Table 1.

of Ar^{2+} at 45.6 nm [9]. The single emission feature with the absence of the other corresponding Rydberg series of lines from Ar^+ confirmed the resonant nonradiative energy transfer of 27.2 eV from atomic hydrogen to Ar^+. The catalysis product, the lower-energy hydrogen atom $H(\frac{1}{2})$, was predicted to be a highly reactive intermediate which further reacts to form the novel hydride ion $H^-(\frac{1}{2})$. This ion was observed spectroscopically at 407 nm corresponding to its predicted binding energy of 3.05 eV. The catalytic reaction is given in Section 1.4.

The EUV spectra (10–60 nm) and (10–65 nm) of the argon–hydrogen mixture ($\frac{90}{10}$%) microwave cell emission are shown in Figs. 7, and 8, respectively. Ordinary hydrogen has no emission in this region as shown in Fig. 4, and no emission below 45 nm was observed with the control argon microwave discharge without hydrogen as shown in Fig. 5. A series of 0.5 eV wide Gaussian-shaped peaks was observed in the spectral region 27–65 nm. The

Table 1
Calculated energies of vibrational transitions of $H_2^*[n=\frac{1}{4};\ n^*=2]^+$ and the observed emission lines

Vibrational quantum number v	Calculated emission (nm) Eqs. (26) (B.80), and (B.119)	Calculated emission (eV) Eq. (26) and (B.119)	Observed lines (nm)	Observed lines (eV)	Difference between experimental and predicted (eV)
0	0	0			
1	1047	1.185			
2	523.3	2.370			
3	348.9	3.555			
4	261.7	4.740			
5	209.3	5.925			
6	174.5	7.110			
7	149.5	8.295			
8	130.8	9.480			
9	116.3	10.67			
10	104.7	11.85			
11	95.15	13.04			
12	87.22	14.22			
13	80.51	15.41			
14	74.76	16.59			
15	69.78	17.78			
16	65.42	18.96			
17	61.57	20.15	61.5	20.2	0.02
18	58.15	21.33	58.1	21.3	0.02
19	55.09	22.52	55.1	22.5	0.00
20	52.33	23.70	52.3	23.7	0.02
21	49.84	24.89	49.8	24.9	0.02
22	47.58	26.07	47.6	26.1	−0.01
23	45.51	27.26	45.5	27.3	0.00
24	43.61	28.44	43.6	28.4	0.01
25	41.87	29.63	41.8	29.7	0.05
26	40.26	30.81	40.2	30.9	0.04
27	38.77	32.00	38.8	32.0	−0.03
28	37.38	33.18	37.4	33.2	−0.02
29	36.09	34.37	36.1	34.4	−0.01
30	34.89	35.55	34.9	35.5	−0.01
31	33.76	36.74	33.8	36.7	−0.04
32	32.71	37.92	32.7	37.9	0.01
33	31.72	39.11	31.7	39.1	0.02
34	30.78	40.29	30.8	40.3	−0.02
35	29.91	41.48	29.9	41.5	0.01
36	29.07	42.66	29.1	42.6	−0.04
37	28.29	43.85	28.3	43.8	−0.02
38	27.54	45.03	27.6	44.9	−0.09

peaks centered on relative increments in energy of 1.185 eV terminated at about 28 nm. $H(1/p)$ may react with a proton to form an excited state molecular ion $H_2^*(1/p)^+$ that has a bond energy and vibrational levels that are p^2 times those of the molecular ion comprising uncatalyzed atomic hydrogen where p is an integer. Ar^+ may serve as a catalyst to form $H(\frac{1}{2})$ which may react with a proton to form $H_2^*[n=\frac{1}{4};n^*=2]^+$. From Eqs. (26) and (B.119), the energy for the $v+1 \rightarrow v$ vibrational transition of $H_2^*[n=\frac{1}{4};n^*=2]^+$ is 1.185 eV. The increment of the McPherson 4° grazing incidence EUV spectrometer was 0.1 nm as described in Section 2. The corresponding energy in this spectral region is about 0.15 eV. The rotational levels given by Eq. (27) could not be resolved since the $J+1 \rightarrow J$ corresponds to 0.03 eV. Thus, the excited state spectrum of $H_2^*[n=\frac{1}{4};n^*=2]^+$ in this region was predicted to comprise rotationally broadened vibrational transitions at 1.185 eV increments (Eq. (26) and Eq. (B.119)) that terminated at about the dissociation limit of $H_2[n=\frac{1}{4}]^+$, $E_D=42.88$ eV(28.92 nm) (Eq. (25)). In Table 1, the novel emission lines were assigned to the $v=17$–38 vibrational

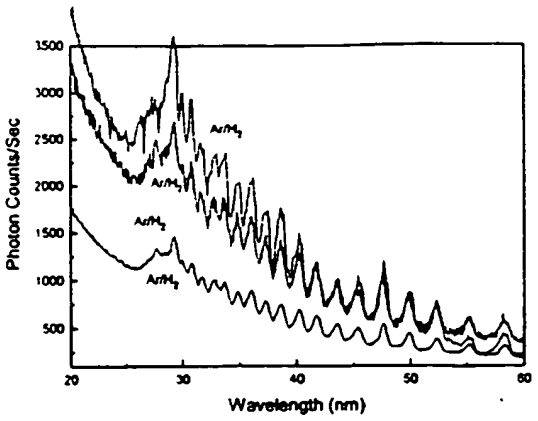

Fig. 9. The three matching EUV spectra (20–60 nm) of the microwave cell emission from argon–hydrogen ($\frac{90}{10\%}$) plasmas that were equivalent to the spectrum shown in Fig. 7.

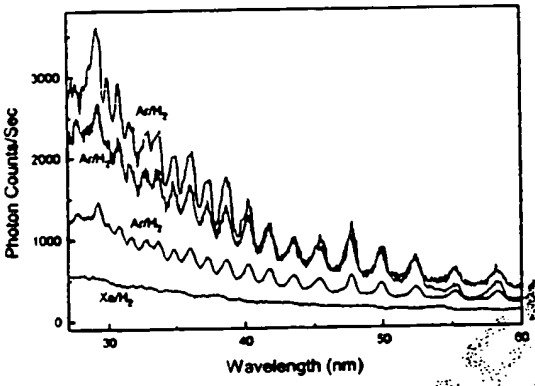

Fig. 10. The three repeatable EUV spectra (27–60 nm) of the microwave cell emission from argon–hydrogen ($\frac{90}{10\%}$) plasmas shown in Fig. 8 with an additional control xenon–hydrogen microwave discharge cell emission that was recorded with a 4° grazing incidence EUV spectrometer and a CEM. No emission was observed in this region from the control.

transitions of $H_2^*[n=\frac{1}{4};n^*=2]^+$ with energies of 1.185 eV that terminated at about 28.9 nm. There is remarkable agreement between the predicted vibrational energies and the observed lines. The unique continuum peak at about 28 nm was the most intense and terminated the series of peaks at the predicted dissociation energy of $H_2[n=\frac{1}{4}]^+$. Thus, this peak was assigned to the dissociation energy of $H_2[n=\frac{1}{4}]^+$. The zero order was extremely intense which corresponded to the observed high intensity of the plasma.

The spectrum of the argon–hydrogen plasma given in Figs. 7 and 8 was found to be very readily reproducible as shown in Figs. 9–11. Fig. 10 shows the region of interest (27–60 nm) of the EUV spectra of the argon–hydrogen plasmas compared to an additional control xenon–hydrogen microwave discharge cell emission. The series of 1.185 eV peaks were not observed from this control or the others shown in Figs. 2–4. Each argon–hydrogen plasmas experiment was performed independently on separate days, and the spectra were essentially identical. The zero order was extremely intense which corresponded to the observed high intensity of the plasma. Often the $H_2^*[n=\frac{1}{4};n^*=2]^+$ vibrational emission was so intense that it dominated or absorbed the electronic emission as shown in Fig. 9 compared to Fig. 11. Other peaks in the latter case were assigned to Ar I and Ar II as shown in Fig. 5.

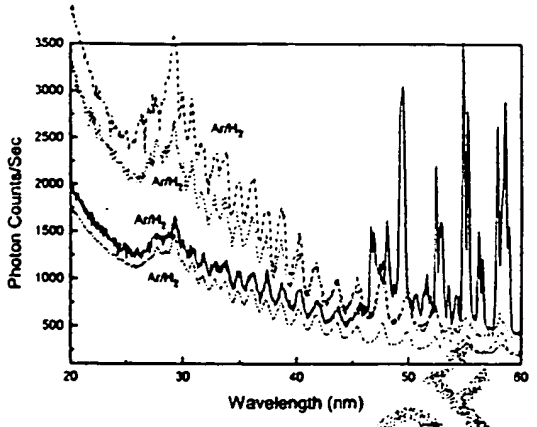

Fig. 11. The three repeatable EUV spectra (20–60 nm) of the microwave cell emission from argon–hydrogen ($\frac{90}{10\%}$) plasmas shown in Fig. 8 wherein the vibrational emission dominated the electronic emission. A fourth repeat spectrum shows other peaks that were assigned to Ar I and Ar II as shown in Fig. 5.

The second ionization energy of helium is 54.4 eV; thus, the ionization reaction of He^+ to He^{2+} has a net enthalpy of reaction of 54.4 eV which is equivalent to 2.272 eV. It was previously reported that EUV spectroscopy was recorded on microwave and glow discharges of helium with 2% hydrogen at 1–760 Torr at a flow rate of 5 sccm wherein helium and the product hydrinos served as catalysts [7]. Novel emission lines were observed with energies of $q13.6$ eV where $q=1,2,3,4,6,7,8,9$, or 11 or these lines inelastically scattered by helium atoms wherein 21.2 eV was absorbed in the excitation of He ($1s^2$) to He ($1s^12p^1$). $H(\frac{1}{3})$, the product with He^+ catalyst, may further serve as a catalyst to form $H(\frac{1}{4})$ and $H(\frac{1}{2})$. The catalysis reaction with He^+ and a favored disproportionation reaction which gives rise to $H(\frac{1}{2})$ are:

$$H[a_H]\xrightarrow{He^+} H\left[\frac{a_H}{3}\right] + 54.4\text{ eV} + 54.4\text{ eV}, \quad (29)$$

$$H\left[\frac{a_H}{3}\right] + H\left[\frac{a_H}{3}\right] \rightarrow H\left[\frac{a_H}{2}\right] + H\left[\frac{a_H}{4}\right] + 27.2\text{ eV}. \quad (30)$$

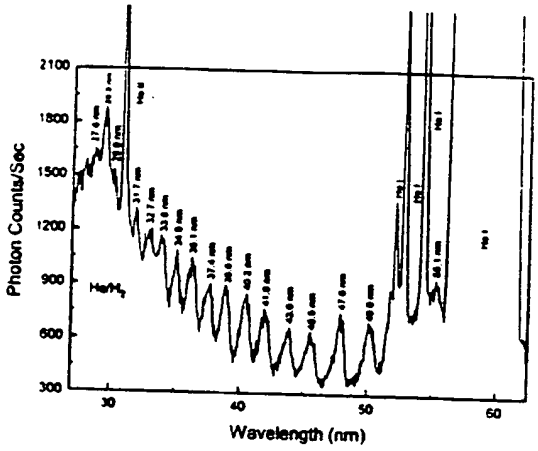

Fig. 12. The EUV spectrum (25–62 nm) of the helium–hydrogen ($\frac{90}{10\%}$) microwave cell emission recorded with 0.1 nm increment of the McPherson 4° grazing incidence EUV spectrometer. A series of 0.5 eV wide Gaussian-shaped peaks were observed in the spectral region 27–55 nm that were assigned to the $v = 19, 21–33, 35–38$ vibrational transitions of $H_2^*[n = \frac{1}{4}; n^* = 2]^+$ with energies $v1.185$ eV as given in Table 1. The intense continuum peak at 28 nm that terminated the series was assigned to the dissociation energy of $H_2[n = \frac{1}{4}]^+$. Other peaks in the helium–hydrogen plasma that covered some of the vibrational peaks shown in Fig. 7 were assigned to He I and He II as shown in Fig. 6.

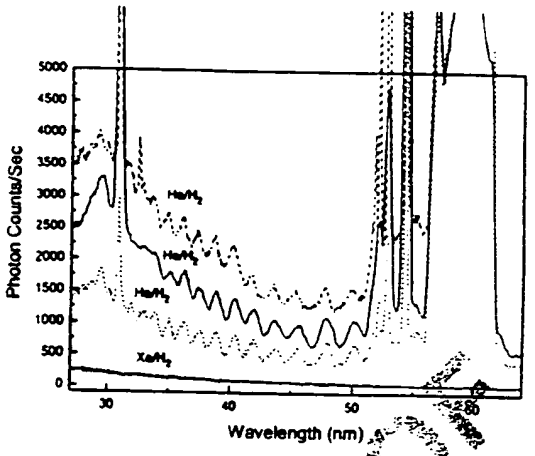

Fig. 13. Three repeatable EUV spectra (27–64 nm) of the microwave cell emission from helium–hydrogen ($\frac{90}{10\%}$) plasmas that were equivalent to the spectrum shown in Fig. 12 with an additional control xenon–hydrogen microwave discharge cell emission that was recorded with a 4° grazing incidence EUV spectrometer and a CEM. No emission was observed in this region from the control.

The latter reaction was confirmed by the intense peak observed at 45.6 nm corresponding to $q13.6$ eV where $q = 2$. As in the case of the Ar^+ catalyst, $H(\frac{1}{2})$ may react with a proton to form $H_2^*[n = \frac{1}{4}; n^* = 2]^+$.

The series of vibrational peaks from the argon–hydrogen plasmas shown in Figs. 7–11 were also observed with the helium ion catalyst. The EUV spectrum (25–62 nm) of the helium–hydrogen ($\frac{90}{10}$%) microwave cell emission with wavelengths assignments is shown in Fig. 12. The EUV spectra (27–64 nm) of the microwave cell emission from three helium-hydrogen ($\frac{90}{10}$%) plasmas with an additional control xenon–hydrogen microwave discharge cell emission are shown in Fig. 13. Each helium–hydrogen experiment was performed independently on separate days. In each case, the series of 0.5 eV wide Gaussian shaped peaks were observed in the spectral region 27–55 nm that were assigned to the $v = 19, 21–33, 35–38$ vibrational transitions of $H_2^*[n = \frac{1}{4}; n^* = 2]^+$ with energies $v1.185$ eV as given in Table 1. The intense continuum peak at about 28 nm that terminated the series was assigned to the dissociation energy of $H_2[n = \frac{1}{4}]^+$. The series of 1.185 eV peaks were not observed from the xenon–hydrogen control shown in Fig. 13 or the other controls shown in Figs. 2–4, and 6. Hydrogen has no emission in this region as shown in Fig. 4. Other peaks in the helium–hydrogen plasma that covered some of the vibrational peaks shown in Fig. 7 were assigned to known intense He I and He II peaks as shown in Fig. 6. In each case, the zero order was extremely intense which corresponded to the observed high intensity of the plasma.

Excited state dihydrino molecular ions other than $H_2^*[n = \frac{1}{4}; n^* = 2]^+$ are predicted to emit outside the measured spectral region at shorter wavelengths, and additional vibrational transitions of $H_2^*[n = \frac{1}{4}; n^* = 2]^+$ are predicted at longer wavelengths as given in Table 1.

2.2. Identification of dihydrino molecules by the assignment of infrared line emissions from the Sun to rotational transitions

The rotational transition energies of lower-energy molecular hydrogen match closely certain spectral lines obtained by Livingston and Wallace [33] using the 1-m Fourier Transform Spectrometer at the McMath telescope on Kitt peak for which no other satisfactory assignment exists. Livingston and Wallace combined infrared solar spectra at different air masses to obtain a solar spectrum in the infrared from 1850 to 9000 cm^{-1} (1.1–5.4 μm) corrected for atmospheric absorption by a point-by-point extrapolation to zero air mass. The spectra were obtained at disk center. The observed region was free of sunspots, and a 1-m out-of-focus image (~ 40 arc-sec diameter area) assured that any surface velocity and brightness structure was averaged over. The spectra band width was set at long wavelengths (~ 5.4 μm) by the response of the InSb detectors and at the short wavelength end (~ 1.1 μm) by a silicon filter. The infrared lines corrected for atmospheric absorption that match the rotational transitions of lower-energy molecular hydrogen are given in Table 2. Similar observations of spectral lines obtained

Table 2
The $J + 1$ to J rotational energy of Solar dihydrino molecules

Observed line wave number (cm^{-1})	Predicted Mills (cm^{-1}) Eq. (27)	p Eq. (B.2)	Assignment Mills Transition $J + 1$ to J Eq. (27)	Ref.	Assignment (other)
1898.2	1898.1	2	4–3	[33]	CO, $\Delta v = 1$ peak
1897.9	1898.1	2	4–3	[34]	None
1894.4					
1898.1	1898.1	2	4–3	[35]	Solar in origin CO
2846.8	2847.1	2	6–5	[33]	None
2847.7	2847.1	2	6–5	[34]	None
2847.1	2847.1	2	6–5	[35]	CH_4 (telluric)
3322	3321.6	2	7–6	[33]	None
3320.4	3321.6	2	7–6	[34]	None
3322					
3321.6	3321.6	2	7–6	[35]	Solar in origin Not identified
4270.8	4270.7	2	9–8	[33]	CO, $\Delta v = 2$ peak
4270.7	4270.7	2	9–8	[34]	None
4745.3	4745.2	2	10–9	[34]	None
1067.7	1067.7	3	1–0	[35]	O_3 (telluric)
2135.3	2135.3	3	2–1	[33]	CO, $\Delta v = 1$ peak
2135.5	2135.3	3	2–1	[34]	None
2135.3	2135.3	3	2–1	[35]	CO (telluric)
3203.1	3203.0	3	3–2	[34]	None
3203.0	3203.0	3	3–2	[35]	Not identified
4270.8	4270.7	3	4–3	[33]	CO, $\Delta v = 2$ peak
4270.7	4270.7	3	4–3	[34]	None
6406.18	6406.0	3	6–5	[33]	Ni, 6406.18
6406.2	6406.0	3	6–5	[34]	None
7473.7	7473.7	3	7–6	[34]	None
8540.9	8541.4	3	8–7	[34]	None
8542.3					
1898.2	1898.1	4	1–0	[33]	CO, $\Delta v = 1$ peak
1897.8	1898.1	4	1–0	[34]	None
1898.4					
5693.8	5694.2	4	3–2	[33]	None
5693.7	5694.2	4	3–2	[34]	None
5694.4					
7592.2	7592.3	4	4–3	[33]	None
7592.6	7592.3	4	4–3	[34]	None
9490.5	9490.4	4	5–4	[34]	None
2967.12	2965.8	5	1–0	[33]	None
2965.7	2965.8	5	1–0	[34]	None
2966					
2965.8	2965.8	5	1–0	[35]	$H_2O, 2\nu_2$ (telluric)
5931.3	5931.5	5	2–1	[33]	None
5931.5	5931.5	5	2–1	[34]	None
8896.7	8897.3	5	3–2	[33]	None
8897.3	8897.3	5	3–2	[34]	None
4270.8	4270.7	6	1–0	[33]	CO, $\Delta v = 2$ peak
4270.7	4270.7	6	1–0	[34]	None
8540.9	8541.4	6	2–1	[34]	None
8542.3					
5812.26	5812.9	7	1–0	[33]	Fe at 5812.26
5814.2					None

Table 2
Continued

Observed line wave number (cm^{-1})	Predicted Mills (cm^{-1}) Eq. (27)	p Eq. (B.2)	Assignment Mills Transition $J+1$ to J Eq. (27)	Ref.	Assignment (other)
5812.7	5812.9	7	1–0	[34]	None
7592.2	7592.3	8	1–0	[33]	None
7592.6	7592.3	8	1–0	[34]	None
60,124	60,142	13	3–2	[36]	Fe(II)
69,783	69,750	14	3–2	[36]	None
53,362	53,381	15	2–1	[36]	Active region unidentified
80,038	80,071	15	3–2	[36]	None
60,710	60,735	16	2–1	[36]	Active region unidentified
68,582	68,564	17	2–1	[36]	S(I)
76,869	76,868	18	2–1	[36]	None

by Brault et al. at Kitt Peak National Observatory [34], M. Migeotte made at Jungfraujoch International Scientific Station of Switzerland [35], and Cohen [36] recorded on Skylab with the NRL's Apollo Telescope also appear in Table 2. The frequency corresponding to the $J+1$ to J rotational transition of the dihydrino molecule (Eq. (B.251) where p is an integer which corresponds to $n=1/p$, the fractional quantum number of the hydrogen-type molecule) are given in Table 2. The assignment of additional lines to rotational transitions of lower-energy hydrogen molecules was limited by the range of the spectrum, the weakness of the spectrum in certain regions, and strong atmospheric components in some regions. The intensity of these forbidden lines supports the possibility of a substantial abundance of dihydrino molecules in the Sun.

4. Conclusion

Transitions to fractional quantum energy levels were previously recorded on microwave and glow discharges of helium with 2% hydrogen. Novel emission lines were observed with energies of $q13.6$ eV where $q=1,2,3,4,6,7,8,9$, or 11 or these lines inelastically scattered by helium atoms wherein 21.2 eV was absorbed in the excitation of He ($1s^2$) to He ($1s^12p^1$) [7]. EUV lines that could be assigned to transitions of atomic hydrogen to lower energy levels corresponding to fractional principal quantum numbers were also previously recorded at the Institut für Niedertemperatur-Plasmaphysik e.V. [15]. Novel hydride compounds were previously reported as final stable products of the catalysis reaction with alkaline or alkaline earth metals or halides as reactants [19–25]. We report that a novel molecular ion corresponding to the diatomic hydrino, dihydrino molecular ion, was observed when noble gas ions Ar^+ or He^+ served as catalysts. Ar^+ may serve as a catalyst to form $H(\frac{1}{2})$. The products of the He^+ catalysis reaction $H(\frac{1}{3})$ may further serve as catalysts to form $H(\frac{1}{4})$ and $H(\frac{1}{5})$. $H(1/p)$ may react with a proton to form an excited state molecular ion $H_2^+(1/p)$ that has a bond energy and vibrational levels that are p^2 times those of the molecular ion comprising uncatalyzed atomic hydrogen where p is an integer. Thus, the excited state spectrum of $H_2^*[n=\frac{1}{4};n^*=2]^+$ was predicted to comprise rotationally broadened vibrational transitions at 1.185 eV increments that terminated at about the dissociation limit of $H_2[n=\frac{1}{4}]^+$, $E_D=42.88$ eV(28.92 nm). EUV spectroscopy was recorded on microwave discharges of argon or helium with 10% hydrogen in the region 10–65 nm. Novel emission lines in this region were assigned to the $v=17$–38 vibrational transitions of $H_2^*[n=\frac{1}{4};n^*=2]^+$ with energies $v1.185$ eV that terminated at about 28.9 nm. Furthermore, astrophysical data was reviewed, and fractional molecular hydrogen rotational transitions were assigned to previously unidentified lines in the Solar coronal spectrum that matched theoretical predictions to five figures. Fractional hydrogen transitions were previously assigned to lines in the Solar EUV spectrum which may resolve the solar neutrino problem, the mystery of the cause of sunspots and other solar activity, and why the Sun emits X-rays [7]. In addition to producing power on the Sun, the catalysis of hydrogen represents a new powerful energy source with the potential for direct conversion of plasma to electricity with the production of novel compounds [26,27]. Helium or argon as the source of catalyst with the formation of stable hydrogen-type molecules offers the possibility of room temperature operation with a gaseous product which may be ventable.

Acknowledgements

Special thanks to Y. Lu and T. Onuma for recording some spectra and B. Dhandapani for assisting with logistics and reviewing this manuscript. Special thanks to J. Farrell for contributions to the analysis of the solar spectral data.

Appendix A. Introduction[1]

A theory of classical quantum mechanics (CQM), derived from first principles, successfully applies physical laws on all scales [1]. The classical wave equation is solved with the constraint that a bound electron cannot radiate energy. The mathematical formulation for zero radiation based on Maxwell's equations follows from a derivation by Haus [37]. The function that describes the motion of the electron must not possess spacetime Fourier components that are synchronous with waves traveling at the speed of light. CQM gives closed form solutions for the atom including the stability of the $n = 1$ state and the instability of the excited states, the equation of the photon and electron in excited states, the equation of the free electron, and photon which predict the wave particle duality behavior of particles and light. The current and charge density functions of the electron may be directly physically interpreted. For example, spin angular momentum results from the motion of negatively charged mass moving systematically, and the equation for angular momentum, $\mathbf{r} \times \mathbf{p}$, can be applied directly to the wave function (a current density function) that describes the electron. The magnetic moment of a Bohr magneton, Stern Gerlach experiment, g factor, Lamb shift, resonant line width and shape, selection rules, correspondence principle, excited states, reduced mass, rotational energies, and momenta, orbital and spin splitting, spin–orbital coupling, Knight shift, and spin–nuclear coupling, ionization of two electron atoms, inelastic electron scattering from helium atoms, and the nature of the chemical bond are derived in closed form equations based on Maxwell's equations. The calculations agree with experimental observations.

A.1. Classical quantum theory

One-electron atoms include the hydrogen atom, He^+, Li^{2+}, Be^{3+}, and so on. The mass-energy and angular momentum of the electron are constant; this requires that the equation of motion of the electron be temporally and spatially harmonic. Thus, the classical wave equation applies and

$$\left[\nabla^2 - \frac{1}{v^2}\frac{\delta^2}{\delta t^2}\right]\rho(r,\theta,\phi,t) = 0, \tag{A.i}$$

where $\rho(r,\theta,\phi,t)$ is the charge density function of the electron in time and space. In general, the wave equation has an infinite number of solutions. To arrive at the solution which represents the electron, a suitable boundary condition must be imposed. It is well known from experiments that each single atomic electron of a given isotope radiates to the same stable state. Thus, Mills chose the physical boundary condition of nonradiation of the bound electron to be imposed on the solution of the wave equation for the charge density function of the electron. The condition for radiation by a moving point charge given by Haus [37] is that its spacetime Fourier transform does possess components that are synchronous with waves traveling at the speed of light. Conversely, it is proposed that the condition for nonradiation by an ensemble of moving point charges that comprises a charge density function is

For non-radiative states, the current-density function must NOT possess spacetime Fourier components that are synchronous with waves traveling at the speed of light.

The Haus derivation applies to a moving charge-density function as well because charge obeys superposition.

From the application of the nonradiative boundary condition, the instability of excited states as well as the stability of the "ground" state arise naturally in the Mills theory as derived in Stability of Atoms and Hydrinos Section [1]. In addition to the above known states of hydrogen (Eq. (1), the theory predicts the existence of a previously unknown form of matter: hydrogen atoms and molecules having electrons of lower energy than the conventional "ground" state, called *hydrinos* and *dihydrinos*, respectively, where each energy level corresponds to a fractional quantum number.

The central field of the proton corresponds to integer one charge. Excited states comprise an electron with a trapped photon. In all energy states of hydrogen, the photon has an electric field which superposes with the field of the proton. In the $n = 1$ state, the sum is one, and the sum is zero in the ionized state. In an excited state, the sum is a fraction of one (i.e. between zero and one). Derivations from first principles given by Mills demonstrate that each "allowed" fraction corresponding to an excited state is 1/integer. The relationship between the electric field equation and the "trapped photon" source charge-density function is given by Maxwell's equation in two dimensions

$$\mathbf{n} \bullet (\mathbf{E}_1 - \mathbf{E}_2) = \frac{\sigma}{\varepsilon_0}, \tag{A.ii}$$

where $\mathbf{n}$ is the radial normal unit vector, $\mathbf{E}_1 = 0$ ($\mathbf{E}_1$ is the electric field outside of the electron), $\mathbf{E}_2$ is given by the total electric field at $r_n = n a_H$, and σ is the surface charge-density. The electric field of an excited state is fractional; therefore, the source charge function is fractional. It is well known that fractional charge is not "allowed". The reason is that fractional charge typically corresponds to a radiative current density function. The excited states of the hydrogen atom are examples. They are radiative; consequently, they are not stable. Thus, an excited electron decays to the first nonradiative state corresponding to an integer field, $n = 1$ (i.e. a field of integer one times the central field of the proton).

Equally valid from first principles are electronic states where the magnitude of the sum of the electric field of the photon and the proton central field are an integer greater than one times the central field of the proton. These states are nonradiative. A catalyst can effect a transition between

[1] All other sections than those given in this Appendix and equations of the type#.# correspond to those given in reference one.

these states via a nonradiative energy transfer. Substantial experimental evidence exists that supports the existence of this novel hydrogen chemistry and its applications [7–27]. Laboratory experiments that confirm the novel hydrogen chemistry include EUV spectroscopy [7–18], characteristic emission from catalysis and the hydride ion products [8,9], lower-energy hydrogen emission [7–9], plasma formation [8,9,12–14,16–18], Balmer α line broadening [10], anomalous plasma afterglow duration [16,17], power generation [10,11,18], and analysis of chemical compounds [19–25].

Appendix B The nature of the chemical bond of hydrogen-type molecules and molecular ions

Two hydrogen atoms react to form a diatomic molecule, the hydrogen molecule

$$2H[a_H] \rightarrow H_2[2c' = \sqrt{2}a_0], \tag{B.1}$$

where $2c'$ is the internuclear distance. Also, two hydrino atoms react to form a diatomic molecule, a dihydrino molecule

$$2H\left[\frac{a_H}{p}\right] \rightarrow H_2\left[2c' = \frac{\sqrt{2}a_0}{p}\right], \tag{B.2}$$

where p is an integer.

Hydrogen molecules form hydrogen molecular ions when they are singly ionized

$$H_2[2c' = \sqrt{2}a_0] \rightarrow H_2[2c' = 2a_0]^+ + e^-. \tag{B.3}$$

Also, dihydrino molecules form dihydrino molecular ions when they are singly ionized

$$H_2\left[2c' = \frac{\sqrt{2}a_0}{p}\right] \rightarrow H_2\left[2c' = \frac{2a_0}{p}\right]^+ + e^-. \tag{B.4}$$

B.1. Hydrogen-type molecular ions

Each hydrogen-type molecular ion comprises two protons and an electron where the equation of motion of the electron is determined by the central field which is p times that of a proton at each focus (p = one for the hydrogen molecular ion, and p is an integer greater than one for each dihydrino molecular ion). The differential equations of motion in the case of a central field are

$$m(\ddot{r} - r\dot{\theta}^2) = f(r), \tag{B.5}$$

$$m(2\dot{r}\dot{\theta} + r\ddot{\theta}) = 0. \tag{B.6}$$

The second or transverse equation, Eq. (A.6), gives the result that the angular momentum is constant

$$r^2\dot{\theta} = \text{constant} = L/m, \tag{B.7}$$

where L is the angular momentum ($\hbar$ in the case of the electron). The central force equations can be transformed into an orbital equation by the substitution, $u = 1/r$. The differential equation of the orbit of a particle moving under a central force is

$$\frac{\delta^2 u}{\delta\theta^2} + u = \frac{-1}{mL^2u^2/m^2} f(u^{-1}). \tag{B.8}$$

Because the angular momentum is constant, motion in only one plane need be considered; thus, the orbital equation is given in polar coordinates. The solution of Eq. (B.8) for an inverse-squared force

$$f(r) = -\frac{k}{r^2} \tag{B.9}$$

is

$$r = r_0\frac{1+e}{1+e\cos\theta}, \tag{B.10}$$

$$e = A\frac{mL^2/m^2}{k}, \tag{B.11}$$

$$r_0 = \frac{mL^2/m^2}{k(1+e)}, \tag{B.12}$$

where e is the eccentricity of the ellipse and A is a constant. The equation of motion due to a central force can also be expressed in terms of the energies of the orbit. The square of the speed in polar coordinates is

$$v^2 = (\dot{r}^2 + r^2\dot{\theta}^2). \tag{B.13}$$

Since a central force is conservative, the total energy, E, is equal to the sum of the kinetic, T, and the potential, V, and is constant. The total energy is

$$\tfrac{1}{2}m(\dot{r}^2 + r^2\dot{\theta}^2) + V(r) = E = \text{constant}. \tag{B.14}$$

Substitution of the variable $u = 1/r$ and Eq. (B.7) into Eq. (B.14) gives the orbital energy equation

$$\frac{1}{2}mL^2/m^2\left[\left(\frac{\delta^2 u}{\delta\theta^2}\right) + u^2\right] + V(u^{-1}) = E. \tag{B.15}$$

Because the potential energy function $V(r)$ for an inverse-squared force field is

$$V(r) = -\frac{k}{r} = -ku \tag{B.16}$$

the energy equation of the orbit, Eq. (B.15),

$$\frac{1}{2}mL^2/m^2\left[\left(\frac{\delta^2 u}{\delta\theta^2}\right) + u^2\right] - ku = E, \tag{B.17}$$

which has the solution

$$r = \frac{m(L^2/m^2)k^{-1}}{1 + [1 + 2Em(L^2/m^2)k^{-2}]^{1/2}\cos\theta}, \tag{B.18}$$

where the eccentricity, e, is

$$e = \left[1 + 2Em\frac{L^2}{m^2}k^{-2}\right]^{1/2}. \quad \text{(B.19)}$$

Eq. (B.19) permits the classification of the orbits according to the total energy, E, as follows:

$E < 0$, $e < 1$ closed orbits (ellipse or circle),

$E = 0$, $e = 1$ parabolic orbit,

$E > 0$, $e > 1$ hyperbolic orbit.

Since $E = T + V$ and is constant, the closed orbits are those for which $T < |V|$, and the open orbits are those for which $T \geqslant |V|$. It can be shown that the time average of the kinetic energy, $\langle T\rangle$, for elliptic motion in an inverse-squared field is $\frac{1}{2}$ that of the time average of the potential energy, $\langle V\rangle$. $\langle T\rangle = \frac{1}{2}\langle V\rangle$.

As demonstrated in the One Electron Atom section of Mills [1], the electric inverse-squared force is conservative; thus, the angular momentum of the electron, $\hbar$, and the energy of atomic orbitspheres (orbitsphere refers to the function which represents the bound electron) is constant. In addition, the orbitspheres are nonradiative when the boundary condition is met.

The central force equation, Eq. (B.14), has orbital solutions which are circular, elliptic, parabolic, or hyperbolic. The former two types of solutions are associated with atomic and molecular orbitals. These solutions are nonradiative. The boundary condition for nonradiation given in the One Electron Atom section, is the absence of components of the space-time Fourier transform of the charge-density function synchronous with waves traveling at the speed of light. The boundary condition is met when the velocity for every point on the orbitsphere is

$$v_n = \frac{\hbar}{m_e r_n}. \quad \text{(B.20)}$$

The allowed velocities and angular frequencies are related to r_n by

$$v_n = r_n\omega_n, \quad \text{(B.21)}$$

$$\omega_n = \frac{\hbar}{m_e r_n^2}. \quad \text{(B.22)}$$

As demonstrated in the One Electron Atom section and by Eq. (B.22), this condition is met for the product function of a radial Dirac delta function and a time harmonic function where the angular frequency, ω, is constant and given by Eq. (B.22),

$$\omega_n = \frac{\hbar}{m_e r_n^2} = \frac{\pi L/m_e}{A}, \quad \text{(B.23)}$$

where L is the angular momentum and A is the area of the closed geodesic orbit. Consider the solution of the central force equation comprising the product of a two-dimensional ellipsoid and a time harmonic function. The spatial part of the product function is the convolution of a radial Dirac delta function with the equation of an ellipsoid. The Fourier transform of the convolution of two functions is the product of the individual Fourier transforms of the functions; thus, the boundary condition is met for an ellipsoidal-time harmonic function when

$$\omega_n = \frac{\pi\hbar}{m_e A} = \frac{\hbar}{m_e ab}, \quad \text{(B.24)}$$

where the area of an ellipse is

$$A = \pi ab, \quad \text{(B.25)}$$

where $2b$ is the length of the semiminor axis and $2a$ is the length of the semimajor axis. The geometry of molecular hydrogen is elliptic with the internuclear axis as the principal axis; thus, the electron orbital is a two-dimensional ellipsoidal-time harmonic function. The mass follows geodesics time harmonically as determined by the central field of the protons at the foci. Rotational symmetry about the internuclear axis further determines that the orbital is a prolate spheroid. In general, ellipsoidal orbits of molecular bonding, hereafter referred to as ellipsoidal molecular orbitals (MOs), have the general equation

$$\frac{x^2}{a^2} + \frac{y^2}{b^2} + \frac{z^2}{c^2} = 1. \quad \text{(B.26)}$$

The semiprincipal axes of the ellipsoid are a, b, c.

In ellipsoidal coordinates the Laplacian is

$$(\eta - \xi)R_\xi\frac{\partial}{\partial\xi}\left(R_\xi\frac{\partial\phi}{\partial\xi}\right) + (\zeta - \xi)R_\eta\frac{\partial}{\partial\eta}\left(R_\eta\frac{\partial\phi}{\partial\eta}\right) + (\xi - \eta)R_\zeta\frac{\partial}{\partial\zeta}\left(R_\zeta\frac{\partial\phi}{\partial\zeta}\right) = 0. \quad \text{(B.27)}$$

An ellipsoidal MO is equivalent to a charged conductor whose surface is given by Eq. (B.26). It carries a total charge q, and its potential is a solution of the Laplacian in ellipsoidal coordinates, Eq. (B.27).

Excited states of orbitspheres are discussed in the Excited States of the One Electron Atom (Quantization) section. In the case of ellipsoidal MOs, excited electronic states are created when photons of discrete frequencies are trapped in the ellipsoidal resonator cavity of the MO. The photon changes the effective charge at the MO surface where the central field is ellipsoidal and arises from the protons and the effective charge of the "trapped photon" at the foci of the MO. Force balance is achieved at a series of ellipsoidal equipotential two-dimensional surfaces confocal with the ground state ellipsoid. The "trapped photons" are solutions of the Laplacian in ellipsoidal coordinates, Eq. (B.27).

As is the case with the orbitsphere, higher and lower energy states are equally valid. The photon standing wave in both cases is a solution of the Laplacian in ellipsoidal coordinates. For an ellipsoidal resonator cavity, the relationship between an allowed circumference, $4aE$, and the photon standing wavelength, λ, is

$$4aE = n\lambda, \quad \text{(B.28)}$$

where n is an integer and where

$$k = \frac{\sqrt{a^2 - b^2}}{a} \tag{B.29}$$

is used in the elliptic integral E of Eq. (B.28). Applying Eqs. (B.28) and (B.29), the relationship between an allowed angular frequency given by Eq. (B.24) and the photon standing wave angular frequency, ω, is

$$\frac{\pi\hbar}{m_e A} = \frac{\hbar}{m_e n a_1 n b_1} = \frac{\hbar}{m_e a_n b_n} = \frac{1}{n^2}\omega_1 = \omega_n, \tag{B.30}$$

where $n = 1, 2, 3, 4, \ldots$

$$n = \tfrac{1}{2}, \tfrac{1}{3}, \tfrac{1}{4}, \ldots,$$

ω_1 is the allowed angular frequency for $n = 1$, a_1 and b_1 are the allowed semimajor and semiminor axes for $n = 1$.

Let us compute the potential of an ellipsoidal MO which is equivalent to a charged conductor whose surface is given by Eq. (B.26). It carries a total charge q, and we assume initially that there is no external field. We wish to know the potential, ϕ, and the distribution of charge, σ, over the conducting surface. To solve this problem a potential function must be found which satisfies Eq. (B.27), which is regular at infinity, and which is constant over the given ellipsoid. Now ξ is the parameter of a family of ellipsoids all confocal with the standard surface $\xi = 0$ whose axes have the specified values a, b, c. The variables ζ and η are the parameters of confocal hyperboloids and as such serve to measure position on any ellipsoid $\xi =$ constant. On the surface $\xi = 0$; therefore, ϕ must be independent of ζ and η. If we can find a function depending only on ξ which satisfies Eq. (B.27) and behaves properly at infinity, it can be adjusted to represent the potential correctly at any point outside the ellipsoid $\xi = 0$.

Let us assume, then, that $\phi = \phi(\xi)$. The Laplacian reduces to

$$\frac{\delta}{\delta\xi}\left(R_\ell \frac{\partial\phi}{\partial\xi}\right) = 0, \quad R_\ell = \sqrt{(\xi + a^2)(\xi + b^2)(\xi + c^2)} \tag{B.31}$$

which on integration leads to

$$\phi(\xi) = C_1 \int_\xi^\infty \frac{\delta\xi}{R_\ell}, \tag{B.32}$$

where C_1 is an arbitrary constant. The choice of the upper limit is such as to ensure the proper behavior at infinity. When ξ becomes very large, R_ℓ approaches $\xi^{3/2}$ and

$$\phi \sim \frac{2C_1}{\sqrt{\xi}} \quad (\xi \to \infty) \tag{B.33}$$

On the other hand, the equation of an ellipsoid can be written in the form

$$\frac{x^2}{1 + a^2/\xi} + \frac{y^2}{1 + b^2/\xi} + \frac{z^2}{1 + c^2/\xi} = \xi. \tag{B.34}$$

If $r^2 = x^2 + y^2 + z^2$ is the distance from the origin to any point on the ellipsoid ξ, it is apparent that as ξ becomes very large $\xi \to r^2$ and hence at great distances from the origin

$$\phi \sim \frac{2C_1}{r}. \tag{B.35}$$

The solution Eq. (B.32) is, therefore, regular at infinity. Moreover, Eq. (B.35) enables us to determine at once the value of C_1; for it has been shown that whatever the distribution, the dominant term of the expansion at remote points is the potential of a point charge at the origin equal to the total charge of the distribution — in this case q. Hence $C_1 = q/8\pi\varepsilon_0$, and the potential at any point is

$$\phi(\xi) = \frac{q}{8\pi\varepsilon_0}\int_\xi^\infty \frac{\partial\xi}{R_\ell}. \tag{B.36}$$

The equipotential surfaces are the ellipsoids $\xi =$ constant. Eq. (B.36) is a elliptic integral and its values have been tabulated [38].

To obtain the normal derivative we must remember that distance along a curvilinear coordinate u^1 is measured not by du^1 but by $h_1 du^1$. In ellipsoidal coordinates

$$h_1 = \frac{1}{2}\frac{\sqrt{(\xi - \eta)(\xi - \zeta)}}{R_\ell}, \tag{B.37}$$

$$\frac{\delta\phi}{\delta n} = \frac{1}{h_1}\frac{\delta\phi}{\delta\xi} = \frac{-q}{4\pi\varepsilon_0}\frac{1}{\sqrt{(\xi - \eta)(\xi - \zeta)}}. \tag{B.38}$$

The density of charge, σ, over the surface $\xi = 0$ is

$$\sigma = \varepsilon_0\left(\frac{\delta\phi}{\delta n}\right)_{\xi=0} = \frac{q}{4\pi\sqrt{\eta\zeta}}. \tag{B.39}$$

Defining x, y, z in terms of ξ, η, ζ we put $\xi = 0$, it may be easily verified that

$$\frac{x^2}{a^4} + \frac{y^2}{b^4} + \frac{z^2}{c^4} = \frac{\zeta\eta}{a^2 b^2 c^2} \quad (\xi = 0). \tag{B.40}$$

Consequently, the charge-density in rectangular coordinates is

$$\sigma = \frac{q}{4\pi abc}\frac{1}{\sqrt{(x^2/a^4 + y^2/b^4 + z^2/c^4)}}. \tag{B.41}$$

(The mass density function of an MO is equivalent to its charge-density function where m replaces q of Eq. (B.41)). The equation of the plane tangent to the ellipsoid at the point x_0, y_0, z_0 is

$$X\frac{x_0}{a^2} + Y\frac{y_0}{b^2} + Z\frac{z_0}{c^2} = 1, \tag{B.42}$$

where X, Y, Z are running coordinates in the plane. After dividing through by the square root of the sum of the squares of the coefficients of X, Y, and Z, the right member is the distance D from the origin to the tangent plane. That is

$$D = \frac{1}{\sqrt{(x^2/a^4 + y^2/b^4 + z^2/c^4)}} \tag{B.43}$$

so that

$$\sigma = \frac{q}{4\pi abc}D. \tag{B.44}$$

In other words, the surface density at any point on a charged ellipsoidal conductor is proportional to the perpendicular distance from the center of the ellipsoid to the plane tangent to the ellipsoid at the point. The charge is thus greater on the more sharply rounded ends farther away from the origin.

In the case of hydrogen-type molecules and molecular ions, rotational symmetry about the internuclear axis requires that two of the axes be equal. Thus, the MO is a spheroid, and Eq. (B.36) can be integrated in terms of elementary functions. If $a > b = c$, the spheroid is prolate, and the potential is given by

$$\phi = \frac{1}{8\pi\varepsilon_0}\frac{q}{\sqrt{a^2-b^2}}\ln\frac{\sqrt{\xi+a^2}+\sqrt{a^2-b^2}}{\sqrt{\xi+a^2}-\sqrt{a^2-b^2}}. \quad \text{(B.45)}$$

Spheroidal force equations electric force. The spheroidal MO is a two-dimensional surface of constant potential given by Eq. (B.45) for $\xi = 0$. For an isolated electron MO the electric field inside is zero as given by Gauss' Law

$$\int_S \mathbf{E}\,dA = \int_V \frac{\rho}{\varepsilon_0}\,dV, \quad \text{(B.46)}$$

where the charge-density, ρ, inside the MO is zero. Gauss' Law at a two-dimensional surface is

$$\mathbf{n}\cdot(\mathbf{E}_1 - \mathbf{E}_2) = \frac{\sigma}{\varepsilon_0} \quad \text{(B.47)}$$

$\mathbf{E}_2$ is the electric field inside which is zero. The electric field of an ellipsoidal MO is given by substituting σ given by Eq. (B.38) and Eq. (B.39) into Eq. (B.47)

$$\mathbf{E} = \frac{\sigma}{\varepsilon_0} = \frac{q}{4\pi\varepsilon_0}\frac{1}{\sqrt{(\xi-\eta)(\xi-\zeta)}}. \quad \text{(B.48)}$$

The electric field in spheroid coordinates is

$$\mathbf{E} = \frac{q}{8\pi\varepsilon_0}\frac{1}{\sqrt{\xi+a^2}}\frac{1}{\sqrt{\xi+b^2}}\frac{1}{c}\sqrt{\frac{\xi^2-1}{\xi^2-\eta^2}}. \quad \text{(B.49)}$$

From Eq. (B.30), the magnitude of the elliptic field corresponding to a below "ground state" hydrogen-type molecular ion is an integer. The integer is one in the case of the hydrogen molecular ion and an integer greater than one in the case of each dihydrino molecular ion. The central electric force from the two protons, $\mathbf{F}_e$, is

$$\mathbf{F}_e = Ze\mathbf{E} = \frac{p2e^2}{8\pi\varepsilon_0}\frac{1}{\sqrt{\xi+a^2}}\frac{1}{\sqrt{\xi+b^2}}\frac{1}{c}\sqrt{\frac{\xi^2-1}{\xi^2-\eta^2}}, \quad \text{(B.50)}$$

where p is one for the hydrogen molecular ion, and p is an integer greater than one for each dihydrino molecule and molecular ion.

Centripetal force. Each infinitesimal point mass of the electron MO moves along a geodesic orbit of a spheroidal MO in such a way that its eccentric angle, θ, changes at a constant rate. That is $\theta = \omega t$ at time t where ω is a constant, and

$$r(t) = ia\cos\omega t + jb\sin\omega t \quad \text{(B.51)}$$

is the parametric equation of the ellipse of the geodesic. If $\mathbf{a}(t)$ denotes the acceleration vector, then

$$\mathbf{a}(t) = -\omega^2 r(t). \quad \text{(B.52)}$$

In other words, the acceleration is centripetal as in the case of circular motion with constant angular speed ω. The centripetal force, $\mathbf{F}_c$, is

$$\mathbf{F}_c = m\mathbf{a} = -m\omega^2 r(t). \quad \text{(B.53)}$$

Recall that nonradiation results when ω = constant given by Eq. (B.30). Substitution of ω given by Eq. (B.30) into Eq. (B.53) gives

$$\mathbf{F}_c = \frac{-\hbar^2}{m_e a^2 b^2} r(t) = \frac{-\hbar^2}{m_e a^2 b^2} D, \quad \text{(B.54)}$$

where D is the distance from the origin to the tangent plane as given by Eq. (B.43). If X is defined as follows:

$$X = \frac{1}{\sqrt{\xi+a^2}}\frac{1}{\sqrt{\xi+b^2}}\frac{1}{c}\sqrt{\frac{\xi^2-1}{\xi^2-\eta^2}} \quad \text{(B.55)}$$

Then, it follows from Eqs. (B.38), (B.44), (B.48), and (B.50) that

$$D = 2ab^2 X. \quad \text{(B.56)}$$

B.1. Force balance of hydrogen-type molecular ions

Force balance between the electric and centripetal forces is

$$\frac{\hbar^2}{m_e a^2 b^2} 2ab^2 X = \frac{pe^2}{4\pi\varepsilon_0} X, \quad \text{(B.57)}$$

which has the parametric solution given by Eq. (B.51) when

$$a = \frac{2a_0}{p}. \quad \text{(B.58)}$$

B.1.2. Energies of hydrogen-type molecular ions

From Eq. (B.30), the magnitude of the elliptic field corresponding to a below "ground state" hydrogen-type molecule is an integer, p. The potential energy, V_e, of the electron MO in the field of magnitude p times that of the protons at the foci ($\xi = 0$) is

$$V_e = \frac{-4pe^2}{8\pi\varepsilon_0\sqrt{a^2-b^2}}\ln\frac{a+\sqrt{a^2-b^2}}{a-\sqrt{a^2-b^2}}, \quad \text{(B.59)}$$

where

$$\sqrt{a^2-b^2} = c' \quad \text{(B.60)}$$

$2c'$ is the distance between the foci which is the internuclear distance. The kinetic energy, T, of the electron MO is given

by the integral of the left-hand side of Eq. (B.57)

$$T = \frac{2\hbar^2}{m_e a\sqrt{a^2-b^2}} \ln \frac{a+\sqrt{a^2-b^2}}{a-\sqrt{a^2-b^2}}. \quad \text{(B.61)}$$

From the orbital equations in polar coordinates, Eqs. (B.10)–(12), the following relationship can be derived:

$$a = \frac{mL^2/m^2}{k(1-e^2)}. \quad \text{(B.62)}$$

For any ellipse,

$$b = a\sqrt{1-e^2}. \quad \text{(B.63)}$$

Thus,

$$b = a\sqrt{\frac{(L^2/m^2)m}{ka}} \quad \text{(polar coordinates)}. \quad \text{(B.64)}$$

Using Eqs. (B.54) and (B.61), and (B.16) and (B.61), respectively, it can be appreciated that b of polar coordinates corresponds to $c' = \sqrt{a^2-b^2}$ of elliptic coordinates, and k of polar coordinates with one attracting focus is replaced by $2k$ of elliptic coordinates with two attracting foci. In elliptic coordinates, k is given by Eq. (B.48) and (B.50)

$$k = \frac{2pe^2}{4\pi\varepsilon_0} \quad \text{(B.65)}$$

and L for the electron equals $\hbar$; thus, in elliptic coordinates

$$c' = a\sqrt{\frac{\hbar^2 4\pi\varepsilon_0}{me^2 2pa}} = \sqrt{\frac{aa_0}{2p}}. \quad \text{(B.66)}$$

Substitution of a given by Eq. (B.58) into Eq. (B.66) is

$$c' = \frac{a_0}{p}. \quad \text{(B.67)}$$

The internuclear distance from Eq. (B.67) is $2c' = 2a_0/p$. One-half the length of the semiminor axis of the prolate spheroidal MO, $b = c$, is

$$b = \sqrt{a^2-c'^2}. \quad \text{(B.68)}$$

Substitution of $a = 2a_0/p$ and $c' = a_0/p$ into Eq. (B.68) is

$$b = \frac{\sqrt{3}}{p}a_0. \quad \text{(B.69)}$$

The eccentricity, e, is

$$e = \frac{c'}{a}. \quad \text{(B.70)}$$

Substitution of $a = 2a_0/p$ and $c' = a_0/p$ into Eq. (B.70) is

$$e = \tfrac{1}{2}. \quad \text{(B.71)}$$

The potential energy, V_p, due to proton–proton repulsion in the field of magnitude p times that of the protons at the foci ($\xi = 0$) is

$$V_p = \frac{pe^2}{8\pi\varepsilon_0\sqrt{a^2-b^2}}. \quad \text{(B.72)}$$

Substitution of a and b given by Eqs. (B.58) and (B.69), respectively, into Eqs. (B.59), (B.61), and (B.72) is

$$V_e = \frac{-4p^2e^2}{8\pi\varepsilon_0 a_0}\ln 3, \quad \text{(B.73)}$$

$$V_p = \frac{p^2e^2}{8\pi\varepsilon_0 a_0}, \quad \text{(B.74)}$$

$$T = \frac{2p^2e^2}{8\pi\varepsilon_0 a_0}\ln 3, \quad \text{(B.75)}$$

$$E_T = V_e + V_p + T, \quad \text{(B.76)}$$

$$E_T = 13.6\ \text{eV}(-4p^2\ln 3 + p^2 + 2p^2\ln 3)$$

$$= -p^2 16.28\ \text{eV}. \quad \text{(B.77)}$$

The bond dissociation energy, E_D, is the difference between the total energy of the corresponding hydrogen atom or hydrino atom and E_T

$$E_D = E\left(\mathrm{H}\left[\frac{a_H}{p}\right]\right) - E_T$$

$$= -p^2 13.6 + p^2 16.28\ \text{eV} = p^2 2.68\ \text{eV}. \quad \text{(B.78)}$$

B.1.3. Vibration of hydrogen-type molecular ions

An oscillating charge $\mathbf{r}_0(t) = \mathbf{d}\sin\omega_0 t$ has a Fourier spectrum

$$J(k,\omega) = \frac{q\omega_0 d}{2}\sum_{m=-\infty}^{\infty} J_m(k\cos\theta d)\{\delta[\omega-(m+1)\omega_0] + \delta[\omega-(m-1)\omega_0]\}, \quad \text{(B.79)}$$

where $J_m's$ are Bessel functions of order m. These Fourier components can, and do, acquire phase velocities that are equal to the velocity of light [37]. The protons of hydrogen-type molecular ions and molecules oscillate as simple harmonic oscillators; thus, vibrating protons will radiate. Moreover, nonoscillating protons may be excited by one or more photons that are resonant with the oscillatory resonance frequency of the molecule or molecular ion, and oscillating protons may be further excited to higher energy vibrational states by resonant photons. The energy of a photon is quantized according to Planck's equation

$$E = \hbar\omega = h\frac{c}{\lambda}. \quad \text{(B.80)}$$

The energy of a vibrational transition corresponds to the energy difference between the initial and final vibrational states. Each state has an electromechanical resonance frequency, and the emitted or absorbed photon is resonant with the difference in frequencies. Thus, as a general principle, quantization of the vibrational spectrum is due to the quantized energies of photons and the electromechanical resonance of the vibrationally excited ion or molecule.

It can be shown that a perturbation of the orbit determined by an inverse-squared force results in simple harmonic

oscillatory motion of the orbit [39]. In a circular orbit in spherical coordinates, the transverse equation of motion gives

$$\dot{\theta} = \frac{L/m}{r^2}. \tag{B.81}$$

where L is the angular momentum. The radial equation of motion is

$$m(\ddot{r} - r\dot{\theta}^2) = f(r). \tag{B.82}$$

Substitution of Eq. (B.81) into Eq. (B.82) gives

$$m\ddot{r} - \frac{m(L/m)^2}{r^3} = f(r). \tag{B.83}$$

For a circular orbit, r is a constant and $\ddot{r} = 0$. Thus, the radial equation of motion is given by

$$-\frac{m(L/m)^2}{a^3} = f(a), \tag{B.84}$$

where a is the radius of the circular orbit for central force $f(a)$ at $r = a$. A perturbation of the radial motion may be expressed in terms of a variable x defined by

$$x = r - a. \tag{B.85}$$

The differential equation can then be written as

$$m\ddot{x} - m(L/m)^2(x + a)^{-3} = f(x + a). \tag{B.86}$$

Expanding the two terms involving $x + a$ as a power series in x, gives

$$m\ddot{x} - m(L/m)^2 a^{-3}\left(1 - 3\frac{x}{a} + \cdots\right) = f(a) + f'(a)x + \cdots. \tag{B.87}$$

Substitution of Eq. (B.84) into Eq. (B.87) and neglecting terms involving x^2 and higher powers of x gives

$$m\ddot{x} + \left[\frac{-3}{a}f(a) - f'(a)\right]x = 0. \tag{B.88}$$

For an inverse-squared central field, the coefficient of x in Eq. (B.88) is positive, and the equation is the same as that of the simple harmonic oscillator. In this case, the particle, if perturbed, oscillates harmonically about the circle $r = a$, and an approximation of the angular frequency of this oscillation is

$$\omega = \sqrt{\frac{[(-3/a)f(a) - f'(a)]}{m}} = \sqrt{\frac{k}{m}}. \tag{B.89}$$

An apsis is a point in an orbit at which the radius vector assumes an extremal value (maximum or minimum). The angle swept out by the radius vector between two consecutive apsides is called the apsidal angle. Thus, the apsidal angle is π for elliptic orbits under the inverse-squared law of force. In the case of a nearly circular orbit, Eq. (B.88) shows that r oscillates about the circle $r = a$, and the period of oscillation is given by

$$\tau_r = 2\pi\sqrt{\frac{m}{-[(3/a)f(a) + f'(a)]}}. \tag{B.90}$$

The apsidal angle in this case is just the amount by which the polar angle θ increases during the time that r oscillates from a minimum value to the succeeding maximum value which is τ_r. From Eq. (B.81), $\dot{\theta} = L/mr^2$, therefore, θ remains constant, and Eq. (B.84) gives

$$\dot{\theta} \approx \frac{L/m}{a^2} = \left[-\frac{f(a)}{ma}\right]^{1/2}. \tag{B.91}$$

Thus, the apsidal angle is given by

$$\psi = \frac{1}{2}\tau_r\dot{\theta} = \pi\left[3 + a\frac{f'(a)}{f(a)}\right]^{-1/2}. \tag{B.92}$$

Thus, the power force of $f(r) = -cr^n$ gives

$$\psi = \pi(3 + n)^{-1/2}. \tag{B.93}$$

The apsidal angle is independent of the size of the orbit in this case. The orbit is re-entrant, or repetitive, in the case of the inverse-squared law ($n = -2$), for which $\psi = \pi$.

In the case of a hydrogen molecule or molecular ion, the electrons which have a mass of $1/1836$ that of the protons move essentially instantaneously. Thus, a stable electron orbit is maintained with oscillatory motion of the protons. Hydrogen molecules and molecular ions are symmetrical along the semimajor axis; thus, the oscillatory motion of protons is along this axis. Let x be the displacement of the protons along the semimajor axis from the position of the initial foci of the stationary state. The equation of proton motion due to the perturbation of an orbit having a central inverse-squared central force [39] and neglecting terms involving x^2 and higher is given by

$$\mu\ddot{x} + kx = 0 \tag{B.94}$$

which has the solution in terms of the maximum amplitude of oscillation of the protons from the initial foci A, the reduced mass μ, the restoring constant or spring constant k, the resonance frequency ω_0, and the vibrational energy E_{vib} [40]

$$A\cos\omega_0 t, \tag{B.95}$$

where

$$\omega_0 = \sqrt{\frac{k}{\mu}}. \tag{B.96}$$

For the two protons which undergo a symmetrical displacement x from the foci, the potential energy corresponding to the oscillation E_{Pvib} is given by

$$E_{Pvib} = 2(\tfrac{1}{2}kx^2) = kx^2. \tag{B.97}$$

The total energy of the oscillating protons $E_{Totalvib}$ is given as the sum of the kinetic and potential energies

$$E_{Totalvib} = \tfrac{1}{2}\mu\dot{x}^2 + kx^2. \tag{B.98}$$

The velocity is zero when x is the maximum amplitude A. The total energy of the oscillating protons $E_{Totalvib}$ is then

given as the potential energy with $x = A$

$$E_{\text{Total vib}} = kA^2. \tag{B.99}$$

Thus,

$$A = \sqrt{\frac{E_{\text{Total vib}}}{k}}. \tag{B.100}$$

It is shown in the Excite States of the One Electron Atom (Quantization) section that the change in angular velocity of the electron orbitsphere, Eq. (2.21), is identical to the angular velocity of the photon necessary for the excitation, ω_{photon} (Eq. (2.19)). The energy of the photon necessary to excite the equivalent transition in an electron orbitsphere is one-half of the excitation energy of the stationary cavity because the change in kinetic energy of the electron orbitsphere supplies one-half of the necessary energy. The change in the angular frequency of the orbitsphere during a transition and the angular frequency of the photon corresponding to the superposition of the free space photon and the photon corresponding to the kinetic energy change of the orbitsphere during a transition are equivalent. The correspondence principle holds. It can be demonstrated that the resonance condition between these frequencies is to be satisfied in order to have a net change of the energy field [41]. The bound electrons are excited with the oscillating protons. Thus, the mechanical resonance frequency ω_0 is only one that of the electromechanical frequency which is equal to the frequency of the free space photon ω which excites the vibrational mode of the hydrogen molecular ion. The vibrational energy E_{vib} corresponding to the photon is given by

$$E_{\text{vib}} = \hbar\omega = \hbar\omega_0 = \hbar\sqrt{\frac{k}{\mu}} = 2kA^2, \tag{B.101}$$

where Planck's equation (Eq. (B.80)) was used. The reduced mass is given by

$$\mu = \frac{m_1 m_2}{m_1 + m_2}. \tag{B.102}$$

Thus,

$$A = \sqrt{\frac{\hbar\omega_0}{2k}}. \tag{B.103}$$

Since the protons are not fixed and vibrate about the center of mass, the maximum amplitude is given by the reduced amplitude A_{reduced} given by

$$A_{\text{reduced}} = \frac{A_1 A_2}{A_1 + A_2} \tag{B.104}$$

where A_n is the amplitude of proton n if the origin is fixed. Thus, Eq. (B.103) becomes

$$A_{\text{reduced}} = \frac{1}{2}\sqrt{\frac{\hbar\omega_0}{2k}} \tag{B.105}$$

and from Eq. (B.96), A_{reduced} is

$$A_{\text{reduced}} \frac{1}{2}\sqrt{\frac{\hbar\omega_0}{2k}} = \frac{1}{2}\sqrt{\frac{\hbar}{2k}}\left(\frac{k}{\mu}\right)^{1/4} = \frac{\sqrt{\hbar}}{2^{3/2}(k\mu)^{1/4}}. \tag{B.106}$$

The total energy of a hydrogen-type molecular ion is given by substituting Eqs. (B.59), (B.61), and (B.72) into Eq. (B.76)

$$\begin{aligned} E_T &= V_e + V_p + T \\ &= \frac{-4pe^2}{8\pi\varepsilon_0\sqrt{a^2-b^2}}\ln\frac{a+\sqrt{a^2-b^2}}{a-\sqrt{a^2-b^2}} + \frac{pe^2}{8\pi\varepsilon_0\sqrt{a^2-b^2}} \\ &\quad + \frac{2\hbar^2}{m_e a\sqrt{a^2-b^2}}\ln\frac{a+\sqrt{a^2-b^2}}{a-\sqrt{a^2-b^2}} \\ &= \left[\frac{2\hbar^2}{m_e a} - \frac{4pe^2}{8\pi\varepsilon_0}\right]\frac{1}{\sqrt{a^2-b^2}}\ln\frac{a+\sqrt{a^2-b^2}}{a-\sqrt{a^2-b^2}} \\ &\quad + \frac{pe^2}{8\pi\varepsilon_0\sqrt{a^2-b^2}}. \end{aligned} \tag{B.107}$$

From Eq. (B.68), the internuclear distance $2c'$ is given by

$$2c' = 2\sqrt{a^2-b^2} \tag{B.108}$$

A hydrogen-type molecular ion comprises two nuclei at the foci and an electron at a prolate spheroid MO. To conserve momentum, the oscillation of the molecular ion comprises a time averaged increase in the internuclear distance with a time-averaged increase in the semiminor axis. This corresponds to motion of the nuclei in phase with the electron. The total energy is a function of the semimajor axis a and c'. The displacement x corresponds to the amplitude of the time averaged increase in the distance from the origin to each focus c' with a time averaged semimajor axis a. Thus, the perturbated internuclear distance $2c''$ is given by

$$2c'' = 2(c' + x) = 2(\sqrt{a^2-b^2} + x). \tag{B.109}$$

The relationship between $2c''$ and the perturbated semimajor axis a' follows from Eq. (B.66)

$$c'' = c' + x = a'\sqrt{\frac{\hbar^2 4\pi\varepsilon_0}{me^2 2pa'}} = \sqrt{\frac{a'a_0}{2p}}. \tag{B.110}$$

Thus,

$$a' = \frac{2p}{a_0}(c' + x)^2. \tag{B.111}$$

The solution to the force balance equation (Eq. (B.57)) for a is $2a_0/p$, and the solution for c' given by Eq. (B.67) is

$$c' = \frac{a_0}{p}. \tag{B.112}$$

From Eq. (B.107), E_{Tvib}, the total energy including vibration with the perturbated origin-to-nucleus distance c'' and the perturbated semimajor axis a' is given by

$$E_{Tvib} = \left[\frac{2\hbar^2}{m_e a'} - \frac{4pe^2}{8\pi\varepsilon_0}\right]\frac{1}{c''}\ln\frac{a'+c''}{a'-c''} + \frac{pe^2}{8\pi\varepsilon_0 c''}. \quad (B.113)$$

Substitution of Eqs. (A.12.110), (A.111) and (B.111) into Eq. (B.113) gives

$$E_{Tvib} = \left[\frac{2\hbar^2}{m_e\frac{2\rho}{a_0}\left(\frac{a_0}{\rho}+x\right)^2} - \frac{4pe^2}{8\pi\varepsilon_0}\right]\frac{1}{\left(\frac{a_0}{\rho}+x\right)} \ln\frac{\frac{2\rho}{a_0}\left(\frac{a_0}{\rho}+x\right)^2 + \left(\frac{a_0}{\rho}+x\right)}{\frac{2\rho}{a_0}\left(\frac{a_0}{\rho}+x\right)^2 - \left(\frac{a_0}{\rho}+x\right)} + \frac{pe^2}{8\pi\varepsilon_0\left(\frac{a_0}{\rho}+x\right)}, \quad (B.114)$$

$$E_{Tvib} = \left[\frac{p^2\hbar^2}{m_e a_0^2\left(1+\frac{\rho}{a_0}x\right)^2} - \frac{4p^2e^2}{8\pi\varepsilon_0 a_0}\right]\frac{1}{\left(1+\frac{\rho}{a_0}x\right)} \ln\frac{\left(3+\frac{2\rho}{a_0}x\right)}{\left(1+\frac{2\rho}{a_0}x\right)} + \frac{p^2e^2}{8\pi\varepsilon_0 a_0\left(1+\frac{\rho}{a_0}x\right)}, \quad (B.115)$$

$$E_{Tvib} = \frac{p^2 13.6\text{ eV}}{\left(1+\frac{\rho}{a_0}x\right)}\left\{\left[\frac{2}{\left(1+\frac{\rho}{a_0}x\right)^2} - 4\right]\ln\frac{\left(3+\frac{2\rho}{a_0}x\right)}{\left(1+\frac{2\rho}{a_0}x\right)} + 1\right\}. \quad (B.116)$$

The vibrational energy E_{vib} is given by the difference in the total energy of the nonoscillating molecular ion E_T (Eq. (B.77)) and that of the oscillating molecular ion E_{Tvib} (Eq. (B.116))

$$E_{vib} = E_{Tvib} - E_T = p^2 13.6\text{ eV}\left[\frac{1}{\left(1+\frac{\rho}{a_0}x\right)}\right] \times\left[\left[\frac{2}{\left(1+\frac{\rho}{a_0}x\right)^2} - 4\right]\ln\frac{\left(3+\frac{2\rho}{a_0}x\right)}{\left(1+\frac{2\rho}{a_0}x\right)} + 1\right] + 2\ln 3 - 1\Bigg]. \quad (B.117)$$

The maximum displacement x is the reduced amplitude $A_{reduced}$ given by Eq. (B.106). Substitution of $A_{reduced}$ into Eq. (B.117) gives

$$E_{vib} = \hbar\omega_0 = \hbar\sqrt{k/\mu} = p^2 13.6\text{ eV}\left[\frac{1}{\left(1+\frac{\rho}{a_0}\frac{\sqrt{\hbar}}{2^{3/2}(k\mu)^{1/4}}\right)}\right] \left[\left[\frac{2}{\left(1+\frac{\rho}{a_0}\frac{\sqrt{\hbar}}{2^{3/2}(k\mu)^{1/4}}\right)^2} - 4\right]\ln\frac{\left(3+\frac{2\rho}{a_0}\frac{\sqrt{\hbar}}{2^{3/2}(k\mu)^{1/4}}\right)}{\left(1+\frac{2\rho}{a_0}\frac{\sqrt{\hbar}}{2^{3/2}(k\mu)^{1/4}}\right)} + 1\right] + 2\ln 3 - 1\Bigg]. \quad (B.118)$$

A solution to

$$p^2 13.6\text{ eV}\left[\frac{1}{\left(1+\frac{\rho}{a_0}\frac{\sqrt{\hbar}}{2^{3/2}(k\mu)^{1/4}}\right)}\right] \left[\left[\frac{2}{\left(1+\frac{\rho}{a_0}\frac{\sqrt{\hbar}}{2^{3/2}(k\mu)^{1/4}}\right)^2} - 4\right]\ln\frac{\left(3+\frac{2\rho}{a_0}\frac{\sqrt{\hbar}}{2^{3/2}(k\mu)^{1/4}}\right)}{\left(1+\frac{2\rho}{a_0}\frac{\sqrt{\hbar}}{2^{3/2}(k\mu)^{1/4}}\right)} + 1\right] + 2\ln 3 - 1\Bigg] - \hbar\sqrt{\frac{k}{\mu}} = 0 \quad (B.119)$$

found by reiteration is

$$k = p^4 168\text{ Nm}^{-1}. \quad (B.120)$$

A harmonic oscillator is a linear system as given by Eq. (B.94), thus, the resonant vibrational frequencies for hydrogen-type molecular ions with protons given by Eq. (B.96) and Eq. (B.120) for the vibrational transition $v_i \rightarrow v_f$ are

$$\omega_{vf} - \omega_{vi} = \Delta\omega = p^2\sqrt{\frac{v_f^2 k}{\mu}} - p^2\sqrt{\frac{v_i^2 k}{\mu}} = (v_f - v_i)p^2\sqrt{\frac{k}{\mu}} = p^2\sqrt{\frac{168\text{ Nm}^{-1}}{\mu}} = p^2 4.48\times10^{14}\text{ radians/s}, \quad (B.121)$$

where v is an integer. From Planck's equation (Eq. (B.80)) and the vibrational frequencies (Eq. (B.121)), the vibrational energies E_{vib} of hydrogen-type molecular ions are

$$E_{vib} = (v_f - v_i)p^2 0.2962\text{ eV}. \quad (B.122)$$

The experimental vibrational energy of the hydrogen molecular ion [43] is

$$E_{vib} = 0.288 \text{ eV}. \quad \text{(B.123)}$$

The amplitude of oscillation given by Eqs. (B.106) and (B.120) is

$$A = (v_f - v_i)\frac{\sqrt{\hbar}}{2^{3/2}(p^4 168 \text{ Nm}^{-1}\ \mu)^{1/4}}$$
$$= (v_f - v_i)\frac{5.93 \times 10^{-12} \text{ m}}{p}. \quad \text{(B.124)}$$

The energy spacing of each of the transitions of the vibrational spectrum is approximately given by Eq. (B.122). However, slight departure is anticipated as higher states are excited due to the distortion of the molecular ion in these states. The actual transition energy may be calculated from Eq. (B.117) wherein the energy difference corresponds to the initial and final states as opposed to the ground vibrational state and the first vibrational state, and higher order terms in the perturbation series are included.

B.2. Hydrogen-type molecules

B.2.1. Force balance of hydrogen-type molecules

Hydrogen-type molecules comprise two indistinguishable electrons bound by an elliptic field. Each electron experiences a centrifugal force, and the balancing centripetal force (on each electron) is produced by the electric force between the electron and the elliptic electric field and the magnetic force between the two electrons causing the electrons to pair. In the present case of hydrogen-type molecules, if the eccentricity equals $1/\sqrt{2}$, then the vectorial projection of the magnetic force between the electrons, $\sqrt{3/4}$ of Eq. (7.15) of the Two Electron Atom section, is one. The molecules will be solved by self-consistency. Assume $e = 1/\sqrt{2}$, then the force balance equation given by Eq. (7.18) of the Two Electron Atom section and Eq. (B.57) is

$$\frac{\hbar^2}{m_e a^2 b^2} 2ab^2 X = \frac{pe^2}{4\pi\varepsilon_0} X + \frac{\hbar^2}{2m_e b^2} X, \quad \text{(B.125)}$$

$$\frac{2a_0}{pa} - \frac{a_0}{pa} = 1, \quad \text{(B.126)}$$

$$a = \frac{a_0}{p}. \quad \text{(B.127)}$$

Substitution of Eq. (B.127) into (B.66) is

$$c' = \frac{1}{p\sqrt{2}} a_0. \quad \text{(B.128)}$$

Substitution of Eqs. (B.127) and (B.128) into Eq. (B.68) is

$$b = c' = \frac{1}{p\sqrt{2}} a_0. \quad \text{(B.129)}$$

Substitution of Eqs. (B.127) and (B.128) into Eq. (B.70) is

$$e = \frac{1}{\sqrt{2}}. \quad \text{(B.130)}$$

The eccentricity is $1/\sqrt{2}$; thus, the present self-consistent solution which was obtained as a boundary value problem is correct. The internuclear distance given by multiplying Eq. (B.128) by two is $a_0\sqrt{2}/p$.

B.2.2. Energies of hydrogen-type molecules

The energy components defined previously for the molecular ion, Eqs. (B.73)–(12.77), apply in the case of the corresponding molecule. And, each molecular energy component is given by the integral of corresponding force in Eq. (B.125) where each energy component is the total for the two equivalent electrons. The parameters a and b are given by Eqs. (B.127) and (B.129), respectively.

$$V_e = \frac{-2pe^2}{8\pi\varepsilon_0\sqrt{a^2 - b^2}} \ln\frac{a + \sqrt{a^2 - b^2}}{a - \sqrt{a^2 - b^2}}, \quad \text{(B.131)}$$

$$V_p = \frac{p}{8\pi\varepsilon_0}\frac{e^2}{\sqrt{a^2 - b^2}}, \quad \text{(B.132)}$$

$$T = \frac{\hbar^2}{2m_e a\sqrt{a^2 - b^2}} \ln\frac{a + \sqrt{a^2 - b^2}}{a - \sqrt{a^2 - b^2}}. \quad \text{(B.133)}$$

The energy, V_m, corresponding to the magnetic force of Eq. (B.125) is

$$V_m = \frac{-\hbar^2}{4m_e a\sqrt{a^2 - b^2}} \ln\frac{a + \sqrt{a^2 - b^2}}{a - \sqrt{a^2 - b^2}}, \quad \text{(B.134)}$$

$$E_T = V_e + T + V_m + V_p, \quad \text{(B.135)}$$

$$E_T = -13.6 \text{ eV}\left[\left(2p^2\sqrt{2} - p^2\sqrt{2} + \frac{p^2\sqrt{2}}{2}\right)\ln\frac{\sqrt{2}+1}{\sqrt{2}-1} - p^2\sqrt{2}\right] = -p^2 31.63, \quad \text{(B.136)}$$

$$E\left(2H\left[\frac{a_H}{p}\right]\right) = -2p^2 13.6 \text{ eV}. \quad \text{(B.137)}$$

The bond dissociation energy, E_D, is the difference between the total energy of the corresponding hydrogen atoms or hydrino atoms and E_T

$$E_D = E\left(2H\left[\frac{a_H}{p}\right]\right) - E_T = -2p^2 13.6 + p^2 31.63 \text{ eV}$$
$$= p^2 4.43 \text{ eV}. \quad \text{(B.138)}$$

B.2.3. Vibration of hydrogen-type molecules

The vibrational energy levels of hydrogen-type molecules may be solved in the same manner as hydrogen-type

molecular ions given in Section B.1.3. The total energy of a hydrogen-type molecule is given by substituting Eqs. (B.59), (B.61) and (B.72) into Eq. (B.76)

$$E_T = V_e + T + V_m + V_p$$

$$= \frac{-2pe^2}{8\pi\varepsilon_0\sqrt{a^2-b^2}} \ln\frac{a+\sqrt{a^2-b^2}}{a-\sqrt{a^2-b^2}} + \frac{\hbar^2}{2m_e a\sqrt{a^2-b^2}} \ln\frac{a+\sqrt{a^2-b^2}}{a-\sqrt{a^2-b^2}} + \frac{-\hbar^2}{4m_e a\sqrt{a^2-b^2}} \ln\frac{a+\sqrt{a^2-b^2}}{a-\sqrt{a^2-b^2}} + \frac{pe^2}{8\pi\varepsilon_0\sqrt{a^2-b^2}}, \quad (B.139)$$

$$E_T = \left[\frac{\hbar^2}{2m_e a} - \frac{2pe^2}{8\pi\varepsilon_0} - \frac{\hbar^2}{4m_e a}\right] \frac{1}{\sqrt{a^2-b^2}} \ln\frac{a+\sqrt{a^2-b^2}}{a-\sqrt{a^2-b^2}} + \frac{pe^2}{8\pi\varepsilon_0\sqrt{a^2-b^2}}, \quad (B.140)$$

$$E_T = \left[\frac{\hbar^2}{4m_e a} - \frac{2pe^2}{8\pi\varepsilon_0}\right] \frac{1}{\sqrt{a^2-b^2}} \ln\frac{a+\sqrt{a^2-b^2}}{a-\sqrt{a^2-b^2}} + \frac{pe^2}{8\pi\varepsilon_0\sqrt{a^2-b^2}}. \quad (B.141)$$

From Eq. (B.68), the internuclear distance $2c'$ is given by

$$2c' = 2\sqrt{a^2-b^2}. \quad (B.142)$$

Thus, the total energy of the nonoscillating molecule is

$$E_T = \left[\frac{\hbar^2}{4m_e a} - \frac{2pe^2}{8\pi\varepsilon_0}\right] \frac{1}{c'} \ln\frac{a+c'}{a-c'} + \frac{pe^2}{8\pi\varepsilon_0 c'}. \quad (B.143)$$

The relationship between $2c'$ and the semimajor axis a follows from Eq. (B.66)

$$2c' = 2a\sqrt{\frac{\hbar^2 4\pi\varepsilon_0}{me^2 2p a'}} = 2\sqrt{\frac{aa_0}{2p}}. \quad (B.144)$$

Substitution of Eq. (B.144) into Eq. (B.143) gives

$$E_T = \left[\frac{\hbar^2}{4m_e a} - \frac{2pe^2}{8\pi\varepsilon_0}\right] \frac{1}{c'} \ln\frac{\sqrt{\frac{2p}{a_0}a}+1}{\sqrt{\frac{2p}{a_0}a}-1} + \frac{pe^2}{8\pi\varepsilon_0 c'}. \quad (B.145)$$

A hydrogen-type molecule comprises two nuclei at the foci and two indistinguishable electrons at the same prolate spheroid MO. The two electrons are spin-paired with the motion of one electron being the mirror image of that of the other. To conserve momentum, the oscillation of the molecule comprises a time averaged decrease in the internuclear distance and a time averaged increase in the semiminor axis relative to the stationary molecule. This corresponds to in-phase motion of the electrons that is opposite to that of the protons. The total energy is a function of the semimajor axis a and the distance from the origin to each focus c'. The energy terms which are a function of the internuclear distance increase in magnitude and those that depend on the semiminor axis decrease in magnitude. The displacement x corresponds to the amplitude of the time averaged decrease in the distance from the origin to each focus c' and increase the time averaged semimajor axis a. Thus, the perturbated semimajor axis a' is given by

$$a' = a + x. \quad (B.146)$$

From Eq. (B.144), the perturbated origin-to-nucleus distance c'' is given by

$$c'' = \sqrt{\frac{(a-x)a_0}{2p}}. \quad (B.147)$$

From Eqs. (B.145), (B.146), and (B.147), the total energy including vibration with the perturbated origin-to-nucleus distance c'' and the perturbated semimajor axis a' is given by

$$E_{Tvib} = \left[\frac{\hbar^2}{4m_e a'} - \frac{2pe^2}{8\pi\varepsilon_0}\right] \frac{1}{c''} \ln\frac{\sqrt{\frac{2p}{a_0}a'}+1}{\sqrt{\frac{2p}{a_0}a'}-1} + \frac{pe^2}{8\pi\varepsilon_0 c''}. \quad (B.148)$$

The solution to the force balance equation (Eq. (B.125)) for a given by Eq. (B.121) is

$$a = \frac{a_0}{p}. \quad (B.149)$$

From Eq. (B.146)

$$a' = \frac{a_0}{p} + x \quad (B.150)$$

and from Eq. (B.147) and Eq. (B.150)

$$c'' = \sqrt{\frac{(a_0/p - x)a_0}{2p}}. \quad (B.151)$$

Substitution of Eqs. (B.150), and (B.151) into Eq. (B.148) gives

$$E_{Tvib} = \left[\frac{\hbar^2}{4m_e\left(\frac{a_0}{p}+x\right)} - \frac{2pe^2}{8\pi\varepsilon_0}\right] \frac{1}{\sqrt{\frac{\left(\frac{a_0}{p}-x\right)a_0}{2p}}} \ln\frac{\sqrt{\frac{2p}{a_0}\left(\frac{a_0}{p}+x\right)}+1}{\sqrt{\frac{2p}{a_0}\left(\frac{a_0}{p}+x\right)}-1} + \frac{pe^2}{8\pi\varepsilon_0\sqrt{\frac{\left(\frac{a_0}{p}-x\right)a_0}{2p}}}. \quad (B.152)$$

$$E_{Tvib} = \left[\frac{p^2\hbar^2}{4m_e a_0^2\left(1+\frac{p}{a_0}x\right)} - \frac{2p^2e^2}{8\pi\varepsilon_0 a_0}\right] \frac{\sqrt{2}}{\sqrt{\left(1-\frac{p}{a_0}x\right)}} \ln\frac{\sqrt{\frac{2p}{a_0}\left(\frac{a_0}{p}+x\right)}+1}{\sqrt{\frac{2p}{a_0}\left(\frac{a_0}{p}+x\right)}-1} + \frac{\sqrt{2}p^2e^2}{8\pi\varepsilon_0 a_0\sqrt{\left(1-\frac{p}{a_0}x\right)}}. \quad (B.153)$$

$$E_{Tvib} = \frac{\sqrt{2}p^2 13.6\,\text{eV}}{\sqrt{\left(1-\frac{\rho}{a_0}x\right)}}\left[\left[\frac{1/2}{\left(1+\frac{\rho}{a_0}x\right)}-2\right]\ln\frac{\sqrt{\frac{2\rho}{a_0}\left(\frac{a_0}{\rho}+x\right)}+1}{\sqrt{\frac{2\rho}{a_0}\left(\frac{a_0}{\rho}+x\right)}-1}+1\right]. \quad \text{(B.154)}$$

$$E_{Tvib} = \frac{\sqrt{2}p^2 13.6\,\text{eV}}{\sqrt{\left(1-\frac{\rho}{a_0}x\right)}}\left[\left[\frac{1/2}{\left(1+\frac{\rho}{a_0}x\right)}-2\right]\ln\frac{\sqrt{2+\frac{2\rho}{a_0}x}+1}{\sqrt{2+\frac{2\rho}{a_0}x}-1}+1\right]. \quad \text{(B.155)}$$

The vibrational energy E_{vib} is given by the difference in the total energy of the nonoscillating molecule E_T (Eq. (B.136)) and that of the oscillating molecule E_{Tvib} (Eq. (B.155))

$$E_{vib} = E_{Tvib} - E_T = p^2 13.6\,\text{eV}\left[\frac{\sqrt{2}}{\sqrt{\left(1-\frac{\rho}{a_0}x\right)}}\left[\left[\frac{1/2}{\left(1+\frac{\rho}{a_0}x\right)}-2\right]\ln\frac{\sqrt{2+\frac{2\rho}{a_0}x}+1}{\sqrt{2+\frac{2\rho}{a_0}x}-1}+1\right]+\left[\left(\sqrt{2}+\frac{\sqrt{2}}{2}\right)\ln\frac{\sqrt{2}+1}{\sqrt{2}-1}-\sqrt{2}\right]\right]. \quad \text{(B.156)}$$

The maximum displacement x is the reduced amplitude $A_{reduced}$ given by Eq. (B.106). Substitution of $A_{reduced}$ into Eq. (B.156) gives

$$E_{vib} = \hbar\omega_0 = \hbar\sqrt{\frac{k}{\mu}} = p^2 13.6\,\text{eV}\left[\frac{\sqrt{2}}{\sqrt{\left(1-\frac{\rho}{a_0}\frac{\sqrt{\hbar}}{2^{3/2}(k\mu)^{1/4}}\right)}}\left[\left[\frac{1/2}{\left(1+\frac{\rho}{a_0}\frac{\sqrt{\hbar}}{2^{3/2}(k\mu)^{1/4}}\right)}-2\right]\ln\frac{\sqrt{2+\frac{2\rho}{a_0}\frac{\sqrt{\hbar}}{2^{3/2}(k\mu)^{1/4}}}+1}{\sqrt{2+\frac{2\rho}{a_0}\frac{\sqrt{\hbar}}{2^{3/2}(k\mu)^{1/4}}}-1}+1\right]+\left[\left(\sqrt{2}+\frac{\sqrt{2}}{2}\right)\ln\frac{\sqrt{2}+1}{\sqrt{2}-1}-\sqrt{2}\right]\right]. \quad \text{(B.157)}$$

A solution to

$$p^2 13.6\,\text{eV}\left[\frac{\sqrt{2}}{\sqrt{\left(1-\frac{\rho}{a_0}\frac{\sqrt{\hbar}}{2^{3/2}(k\mu)^{1/4}}\right)}}\left[\left[\frac{1/2}{\left(1+\frac{\rho}{a_0}\frac{\sqrt{\hbar}}{2^{3/2}(k\mu)^{1/4}}\right)}-2\right]\ln\frac{\sqrt{2+\frac{2\rho}{a_0}\frac{\sqrt{\hbar}}{2^{3/2}(k\mu)^{1/4}}}+1}{\sqrt{2+\frac{2\rho}{a_0}\frac{\sqrt{\hbar}}{2^{3/2}(k\mu)^{1/4}}}-1}\right]+\left[\left(\sqrt{2}+\frac{\sqrt{2}}{2}\right)\ln\frac{\sqrt{2}+1}{\sqrt{2}-1}-\sqrt{2}\right]\right]-\hbar\sqrt{\frac{k}{\mu}}=0 \quad \text{(B.158)}$$

found by reiteration is

$$k = p^4 570\ \text{Nm}^{-1}. \quad \text{(B.159)}$$

The resonant vibrational frequencies for hydrogen-type molecules with proton nuclei given by Eq. (B.96) and Eq. (B.159) are

$$\omega_0 = p^2\sqrt{\frac{k}{\mu}} = p^2\sqrt{\frac{570\ \text{Nm}^{-1}}{\mu}} = p^2 8.2\times10^{14}\ \text{radians/s}. \quad \text{(B.160)}$$

From Planck's equation (Eq. (B.80) and the vibrational frequencies (Eq. (B.160)), the vibrational energies E_{vib} of hydrogen-type molecules are

$$E_{vib} = p^2 0.543\ \text{eV}. \quad \text{(B.161)}$$

The experimental vibrational energy of the hydrogen molecule [43] is

$$E_{vib} = 0.545\ \text{eV}. \quad \text{(B.162)}$$

The amplitude of oscillation given by Eqs. (B.106) and (B.159) is

$$A = \frac{\sqrt{\hbar}}{2^{3/2}(p^4 570\ \text{Nm}^{-1}\,\mu)^{1/4}} = \frac{4.37\times10^{-12}\ \text{m}}{p}. \quad \text{(B.163)}$$

Due to the pairing of the two electrons, the vibrational energies of hydrogen-type molecules are nonlinear as a function of the vibrational quantum number v. The energy spacing of each of the transitions of the vibrational spectrum is approximately given by Eq. (B.158) wherein the corresponding amplitude of the proton displacement of each state is approximately $vA_{reduced}$. The lines do become more closely spaced as higher states are excited due to the distortion of the molecule in these states. The actual transition energy may be better calculated from Eq. (B.156) wherein the energy difference corresponds to the initial and final states

as opposed to the ground vibrational state and the first vibrational state, and higher order terms in the perturbation series are included.

B.3. The hydrogen molecular ion $H_2[2c' = 2a_0]^+$

B.3.1. Force balance of the hydrogen molecular ion

Force balance between the electric and centripetal forces is given by Eq. (B.57) where $p = 1$

$$\frac{\hbar^2}{m_e a^2 b^2} 2ab^2 X = \frac{e^2}{4\pi\varepsilon_0} X, \tag{B.164}$$

which has the parametric solution given by Eq. (B.51) when

$$a = 2a_0. \tag{B.165}$$

The semimajor axis, a, is also given by Eq. (B.58) where $p = 1$. The internuclear distance, $2c'$, which is the distance between the foci is given by Eq. (B.67) where $p = 1$

$$2c' = 2a_0. \tag{B.166}$$

The experimental internuclear distance is $2a_0$. The semiminor axis is given by Eq. (B.69) where $p = 1$

$$b = \sqrt{3}a_0. \tag{B.167}$$

The eccentricity, e, is given by Eq. (B.71)

$$e = \tfrac{1}{2}. \tag{B.168}$$

B.3.2. Energies of the hydrogen molecular ion

The potential energy, V_e, of the electron MO in the field of the protons at the foci ($\xi = 0$) is given by Eq. (B.69) where $p = 1$

$$V_e = \frac{-4e^2}{8\pi\varepsilon_0\sqrt{a^2 - b^2}} \ln\frac{a + \sqrt{a^2 - b^2}}{a - \sqrt{a^2 - b^2}}. \tag{B.169}$$

The potential energy, V_p, due to proton–proton repulsion is given by Eq. (B.72) where $p = 1$

$$V_p = \frac{e^2}{8\pi\varepsilon_0\sqrt{a^2 - b^2}}. \tag{B.170}$$

The kinetic energy, T, of the electron MO is given by Eq. (B.61) where $p = 1$

$$T = \frac{2\hbar^2}{m_e a\sqrt{a^2 - b^2}} \ln\frac{a + \sqrt{a^2 - b^2}}{a - \sqrt{a^2 - b^2}}. \tag{B.171}$$

Substitution of a and b given by Eqs. (B.165) and (B.167), respectively, into Eqs. (B.169), (B.170), and (B.171) is

$$V_e = \frac{-4e^2}{8\pi\varepsilon_0 a_0} \ln 3 = -59.763 \text{ eV}, \tag{B.172}$$

$$V_p = \frac{e^2}{8\pi\varepsilon_0 a_0} = 13.6 \text{ eV}, \tag{B.173}$$

$$T = \frac{2e^2}{8\pi\varepsilon_0 a_0} \ln 3 = 29.88 \text{ eV}, \tag{B.174}$$

$$E_T = V_e + V_p + T, \tag{B.175}$$

$$E_T = -16.282 \text{ eV}, \tag{B.176}$$

$$E(H[a_H]) = -13.6 \text{ eV},$$

$$E_T = V_e + V_p + T, \tag{B.177}$$

$$E_T = 13.6 \text{ eV}(-4\ln 3 + 1 + 2\ln 3) = -16.28 \text{ eV}. \tag{B.178}$$

The bond dissociation energy, E_D, is the difference between the total energy of the corresponding hydrogen atom and E_T

$$E_D = E\left(H\left[\frac{a_H}{p}\right]\right) - E_T = -13.6 + 16.28 \text{ eV} = 2.68 \text{ eV}. \tag{B.179}$$

Eqs. (B.172)–(12.179) are equivalent to Eqs. (B.73)–(12.78) where $p = 1$. The experimental bond energy of the hydrogen molecular ion [42] is

$$E_D = 2.651 \text{ eV}. \tag{B.180}$$

B.3.3. Vibration of the hydrogen molecular ion

It can be shown that a perturbation of the orbit determined by an inverse-squared force results in simple harmonic oscillator motion of the orbit [39]. The spring constant k for the hydrogen molecular ion with protons given by Eq. (B.120)

$$k = 168 \text{ Nm}^{-1}, \tag{B.181}$$

wherein $p = 1$. The resonant vibrational frequency for the hydrogen molecular ion with protons given by Eq. (B.121) is

$$\omega_0 = \sqrt{\frac{k}{\mu}} = \sqrt{\frac{168 \text{ Nm}^{-1}}{\mu}} = 4.48 \times 10^{14} \text{ radians/s}. \tag{B.182}$$

The vibrational energy E_{vib} of the hydrogen molecular ion given by Eq. (B.122) is

$$E_{vib} = 0.2962 \text{ eV}. \tag{B.183}$$

The experimental vibrational energy of the hydrogen molecular ion [42] is

$$E_{vib} = 0.288 \text{ eV}. \tag{B.184}$$

The amplitude of oscillation given by Eq. (B.124) is

$$A = \frac{\sqrt{\hbar}}{2^{3/2}(168 \text{ Nm}^{-1}\,\mu)^{1/4}} = 5.93 \times 10^{-12} \text{ m}. \tag{B.185}$$

B.4. The hydrogen molecule $H_2[2c' = \sqrt{2}a_0]$

B.4.1. Force balance of the hydrogen molecule

The force balance equation for the hydrogen molecule is given by Eq. (B.125) where $p = 1$

$$\frac{\hbar^2}{m_e a^2 b^2} 2ab^2 X = \frac{e^2}{4\pi\varepsilon_0} X + \frac{\hbar^2}{2m_e a^2 b^2} 2ab^2 X, \tag{B.186}$$

which has the parametric solution given by Eq. (B.51) when

$$a = a_0. \tag{B.187}$$

The semimajor axis, a, is also given by Eq. (B.127) where $p = 1$. The internuclear distance, $2c'$, which is the distance between the foci is given by Eq. (B.128) where $p = 1$

$$2c' = \sqrt{2}a_0. \tag{B.188}$$

The experimental internuclear distance is $\sqrt{2}a_0$. The semiminor axis is given by Eq. (B.129) where $p = 1$

$$b = \frac{1}{\sqrt{2}} a_0. \tag{B.189}$$

The eccentricity, e, is given by Eq. (B.130)

$$e = \frac{1}{\sqrt{2}}. \tag{B.190}$$

The finite dimensions of the hydrogen molecule are evident in the plateau of the resistivity versus pressure curve of metallic hydrogen [43].

B.4.2. Energies of the hydrogen molecule

The energies of the hydrogen molecule are given by Eqs. (B.131)–(12.137) where $p = 1$

$$V_e = \frac{-2e^2}{8\pi\varepsilon_0\sqrt{a^2 - b^2}} \ln\frac{a + \sqrt{a^2 - b^2}}{a - \sqrt{a^2 - b^2}} = -67.813 \text{ eV}, \tag{B.191}$$

$$V_p = \frac{e^2}{8\pi\varepsilon_0\sqrt{a^2 - b^2}} = 19.23 \text{ eV}, \tag{B.192}$$

$$T = \frac{\hbar^2}{2m_e a\sqrt{a^2 - b^2}} \ln\frac{a + \sqrt{a^2 - b^2}}{a - \sqrt{a^2 - b^2}} = 13.906 \text{ eV}. \tag{B.193}$$

The energy, V_m, of the magnetic force is

$$V_m = \frac{-\hbar^2}{4m_e a\sqrt{a^2 - b^2}} \ln\frac{a + \sqrt{a^2 - b^2}}{a - \sqrt{a^2 - b^2}} = -16.9533 \text{ eV}, \tag{B.194}$$

$$E_T = V_e + T + V_m + V_p, \tag{B.195}$$

$$E_T = -13.6 \text{ eV}\left[\left(2\sqrt{2} - \sqrt{2} + \frac{\sqrt{2}}{2}\right) \ln\frac{\sqrt{2}+1}{\sqrt{2}-1} - \sqrt{2}\right] = -31.63 \text{ eV}, \tag{B.196}$$

$$E(2H[a_H]) = -27.21 \text{ eV}. \tag{B.197}$$

The bond dissociation energy, E_D, is the difference between the total energy of the corresponding hydrogen atoms and E_T

$$E_D = E(2H[a_H]) - E_T = -27.2 + 31.63 \text{ eV} = 4.43 \text{ eV}. \tag{B.198}$$

The experimental bond energy of the hydrogen molecule [42] is

$$E_D = 4.478 \text{ eV}. \tag{B.199}$$

B.4.3. Vibration of the hydrogen molecule

It can be shown that a perturbation of the orbit determined by an inverse-squared force results in simple harmonic oscillatory motion of the orbit [39]. The spring constant k for the hydrogen molecule with protons given by Eq. (B.159) is

$$k = 570 \text{ Nm}^{-1}, \tag{B.200}$$

wherein $p = 1$. The resonant vibrational frequency for the hydrogen molecule with protons given by Eq. (B.160) is

$$\omega_0 = \sqrt{\frac{k}{\mu}} = \sqrt{\frac{570 \text{ Nm}^{-1}}{\mu}} = 8.2 \times 10^{14} \text{ radians/s}. \tag{B.201}$$

The vibrational energy E_{vib} of the hydrogen molecule given by Eq. (B.161) is

$$E_{vib} = 0.543 \text{ eV}. \tag{B.202}$$

The experimental vibrational energy of the hydrogen molecule [43] is

$$E_{vib} = 0.545 \text{ eV}. \tag{B.203}$$

The amplitude of oscillation given by Eq. (B.163) is

$$A = \frac{\sqrt{\hbar}}{2^{3/2}(570 \text{ Nm}^{-1}\,\mu)^{1/4}} = 4.37 \times 10^{-12} \text{ m}. \tag{B.204}$$

B.5. The dihydrino molecular ion $H_2[2c' = a_0]^+$

B.5.1. Force balance of the dihydrino molecular ion

Force balance between the electric and centripetal forces is given by Eq. (B.57) where $p = 2$

$$\frac{\hbar^2}{m_e a^2 b^2} 2ab^2 X = \frac{2e^2}{4\pi\varepsilon_0} X, \tag{B.205}$$

which has the parametric solution given by Eq. (B.51) when

$$a = a_0. \tag{B.206}$$

The semimajor axis, a, is also given by Eq. (B.58) where $p = 2$. The internuclear distance, $2c'$, which is the distance

between the foci is given by Eq. (B.67) where $p = 2$

$$2c' = a_0. \tag{B.207}$$

The semiminor axis is given by Eq. (B.69) where $p = 2$

$$b = \frac{\sqrt{3}}{2} a_0. \tag{B.208}$$

The eccentricity, e, is given by Eq. (B.71).

$$e = \frac{1}{2}. \tag{B.209}$$

B.5.2. Energies of the dihydrino molecular ion

The potential energy, V_e, of the electron MO in the field of magnitude twice that of the protons at the foci ($\xi = 0$) is given by Eq. (B.59) where $p = 2$

$$V_e = \frac{-8e^2}{8\pi\varepsilon_0\sqrt{a^2 - b^2}} \ln\frac{a + \sqrt{a^2 - b^2}}{a - \sqrt{a^2 - b^2}}. \tag{B.210}$$

The potential energy, V_p, due to proton–proton repulsion in the field of magnitude twice that of the protons at the foci ($\xi = 0$) is given by Eq. (B.72) where $p = 2$

$$V_p = \frac{2e^2}{8\pi\varepsilon_0\sqrt{a^2 - b^2}}. \tag{B.211}$$

The kinetic energy, T, of the electron MO is given by Eq. (B.61) where $p = 2$

$$T = \frac{2\hbar^2}{m_e a\sqrt{a^2 - b^2}} \ln\frac{a + \sqrt{a^2 - b^2}}{a - \sqrt{a^2 - b^2}}. \tag{B.212}$$

Substitution of a and b given by Eqs. (B.206) and (B.208), respectively, into Eqs. (B.210), (B.211), and (B.212) is

$$V_e = \frac{-16e^2}{8\pi\varepsilon_0 a_0} \ln 3 = -239.058 \text{ eV}, \tag{B.213}$$

$$V_p = \frac{4e^2}{8\pi\varepsilon_0 a_0} = 54.42 \text{ eV}, \tag{B.214}$$

$$T = \frac{8e^2}{8\pi\varepsilon_0 a_0} \ln 3 = 119.53 \text{ eV}, \tag{B.215}$$

$$E\left(\mathrm{H}\left[\frac{a_H}{2}\right]\right) = -54.4 \text{ eV}, \tag{B.216}$$

$$E_T = V_e + V_p + T, \tag{B.217}$$

$$E_T = 13.6 \text{ eV}(-16\ln 3 + 4 + 8\ln 3) = -65.09 \text{ eV}. \tag{B.218}$$

The bond dissociation energy, E_D, is the difference between the total energy of the corresponding hydrino atom and E_T

$$E_D = E\left(\mathrm{H}\left[\frac{a_H}{2}\right]\right) - E_T = -54.4 + 65.09 \text{ eV} = 10.69 \text{ eV}. \tag{B.219}$$

Eqs. (B.213)–(12.219) are equivalent to Eqs. (B.73)–(12.78) where $p = 2$.

B.5.3. Vibration of the dihydrino molecular ion

It can be shown that a perturbation of the orbit determined by an inverse-squared force results in simple harmonic oscillatory motion of the orbit [39]. The spring constant k for the dihydrino molecular ion with protons given by Eq. (B.120) is

$$k = 2^4 168 \text{ Nm}^{-1} = 2688 \text{ Nm}^{-1}, \tag{B.220}$$

wherein $p = 2$. The resonant vibrational frequency for the dihydrino molecular ion with protons given by Eq. (B.121) is

$$\omega_0 = 2^2\sqrt{\frac{k}{\mu}} = 2^2\sqrt{\frac{168 \text{ Nm}^{-1}}{\mu}} = 1.79 \times 10^{15} \text{ radians/s}. \tag{B.221}$$

The vibrational energy E_{vib} of the dihydrino molecular ion given by Eq. (B.122) is

$$E_{vib} = 2^2(0.2962) \text{ eV} = 1.185 \text{ eV}. \tag{B.222}$$

The amplitude of oscillation given by Eq. (B.124) is

$$A = \frac{\sqrt{\hbar}}{2^{3/2}(2^4(168)\text{Nm}^{-1}\mu)^{1/4}} = \frac{5.93 \times 10^{-12} \text{ m}}{2} = 2.97 \times 10^{-12} \text{ m}. \tag{B.223}$$

B.6. The dihydrino molecule $H_2[2c' = a_0/\sqrt{2}]$

B.6.1. Force balance of the dihydrino molecule

The force balance equation for the dihydrino molecule $H_2[2c' = a_0/\sqrt{2}]$ is given by Eq. (B.125) where $p = 2$

$$\frac{\hbar^2}{m_e a^2 b^2} 2ab^2 X = \frac{2e^2}{4\pi\varepsilon_0} X + \frac{\hbar^2}{2m_e a^2 b^2} 2ab^2 X, \tag{B.224}$$

which has the parametric solution given by Eq. (B.51) when

$$a = \frac{a_0}{2}. \tag{B.225}$$

The semimajor axis, a, is also given by Eq. (B.127) where $p = 2$. The internuclear distance, $2c'$, which is the distance between the foci is given by Eq. (B.128) where $p = 2$

$$2c' = \frac{1}{\sqrt{2}} a_0. \tag{B.226}$$

The semiminor axis is given by Eq. (B.129) where $p = 2$

$$b = c = \frac{1}{2\sqrt{2}} a_0. \tag{B.227}$$

The eccentricity, e, is given by Eq. (B.130)

$$e = \frac{1}{\sqrt{2}}. \tag{B.228}$$

B.6.2. Energies of the dihydrino molecule

The energies of the dihydrino molecule $H_2[2c' = a_0/\sqrt{2}]$ are given by Eqs. (B.131)–(12.137) where $p = 2$

$$V_e = \frac{-4e^2}{8\pi\varepsilon_0\sqrt{a^2-b^2}} \ln\frac{a+\sqrt{a^2-b^2}}{a-\sqrt{a^2-b^2}} = -271.23 \text{ eV}, \tag{B.229}$$

$$V_p = \frac{2}{8\pi\varepsilon_0}\frac{e^2}{\sqrt{a^2-b^2}} = 76.93 \text{ eV}, \tag{B.230}$$

$$T = \frac{\hbar^2}{2m_e a\sqrt{a^2-b^2}} \ln\frac{a+\sqrt{a^2-b^2}}{a-\sqrt{a^2-b^2}} = 135.614 \text{ eV}. \tag{B.231}$$

The energy, V_m, of the magnetic force is

$$V_m = \frac{-\hbar^2}{4m_e a\sqrt{a^2-b^2}} \ln\frac{a+\sqrt{a^2-b^2}}{a-\sqrt{a^2-b^2}} = -67.8069 \text{ eV}, \tag{B.232}$$

$$E_T = V_e + T + V_m + V_p, \tag{B.233}$$

$$E_T = -13.6 \text{ eV}\left[\left(8\sqrt{2} - 4\sqrt{2} + \frac{4\sqrt{2}}{2}\right)\ln\frac{\sqrt{2}+1}{\sqrt{2}-1} - 4\sqrt{2}\right] = -126.5 \text{ eV}, \tag{B.234}$$

$$E\left(2H\left[\frac{a_H}{2}\right]\right) = -2(54.4) \text{ eV}. \tag{B.235}$$

The bond dissociation energy, E_D, is the difference between the total energy of the corresponding hydrino atoms and E_T

$$E_D = E\left(2H\left[\frac{a_H}{2}\right]\right) - E_T = -108.8 + 126.5 \text{ eV} = 17.7 \text{ eV}. \tag{B.236}$$

B.6.3. Vibration of the dihydrino molecule

It can be shown that a perturbation of the orbit determined by an inverse-squared force results in simple harmonic oscillatory motion of the orbit [39]. The spring constant k for the dihydrino molecule with protons given by Eq. (B.159) is

$$k = 2^4 570 \text{ Nm}^{-1} = 9120 \text{ Nm}^{-1}, \tag{B.237}$$

wherein $p = 2$. The resonant vibrational frequency for the dihydrino molecule with protons given by Eq. (B.160) is

$$\omega_0 = 2^2\sqrt{\frac{k}{\mu}} = 2^2\sqrt{\frac{570 \text{ Nm}^{-1}}{\mu}} = 3.28 \times 10^{15} \text{ radians/s}. \tag{B.238}$$

The vibrational energy E_{vib} of the dihydrino molecule given by Eq. (B.161) is

$$E_{vib} = 2^2(0.543) \text{ eV} = 2.17 \text{ eV}. \tag{B.239}$$

The amplitude of oscillation given by Eq. (B.163) is

$$A = \frac{\sqrt{\hbar}}{2^{3/2}(2^4(570) \text{ Nm}^{-1}\mu)^{1/4}} = \frac{4.37 \times 10^{-12} \text{ m}}{2} = 2.19 \times 10^{-12} \text{ m}. \tag{B.240}$$

B.7. Diatomic molecular rotation

A molecule with a permanent dipole moment can resonantly absorb a photon which excites a rotational mode about the center of mass of the molecule. Momentum must be conserved with excitation of a rotational mode. The photon carries $\hbar$ of angular momentum; thus, the rotational angular momentum of the molecule changes by $\hbar$. And, the rotational charge-density function is equivalent to the rigid rotor problem considered in the Rotational Parameters of the Electron (Angular Momentum, Rotational Energy, Moment of Inertia) section with the exception that for a diatomic molecule having atoms of masses m_1 and m_2, the moment of inertia is

$$I = \mu r^2, \tag{B.241}$$

where μ is the reduced mass

$$\mu = \frac{m_1 m_2}{m_1 + m_2} \tag{B.242}$$

and where r is the distance between the centers of the atoms, the internuclear distance. The rotational energy levels follow from Eq. (1.95)

$$E_{\text{rotational orbital}} = \frac{\hbar^2}{2I}J(J+1), \tag{B.243}$$

where J is an integer. For Eq. (B.243), $J = 0$ corresponds to rotation about the z-axis where the internuclear axis is along the y-axis, and $J \neq 0$ corresponds to a linear combination of rotations about the z- and x-axis.

As given in the Selection Rules section, the radiation of a multipole of order (l, m) carries $m\hbar$ units of the z component of angular momentum per photon of energy $\hbar\omega$. Thus, the z component of the angular momentum of the corresponding excited rotational state is

$$L_z = m\hbar. \tag{B.244}$$

Thus, the selection rule for rotational transitions is

$$\Delta J = \pm 1. \tag{B.245}$$

In addition, the molecule must posses a permanent dipole moment. In the case of absorption of electromagnetic radiation, the molecule goes from a state with a quantum number J to one with a quantum number of $J + 1$. Using Eq. (B.243), the energy difference is

$$\Delta E = E_{J+1} - E_J = \frac{\hbar^2}{I}[J+1]. \tag{B.246}$$

B.7.1. Diatomic molecular rotation of hydrogen-type molecules

The reduced mass of hydrogen-type molecules, μ_{H_2}, having two protons is given by Eq. (B.242) where $m_1 = m_2 = m_p$, and m_p is the mass of the proton

$$\mu_{H_2} = \frac{m_p m_p}{m_p + m_p} = \frac{1}{2} m_p. \tag{B.247}$$

The moment of inertia of hydrogen-type molecules is given by substitution of the reduced mass, Eq. (B.247), for μ of Eq. (B.241) and substitution of the internuclear distance, two times Eq. (B.128), for r of Eq. (B.241)

$$I = m_p \frac{a_0^2}{p^2}, \tag{B.248}$$

where p is an integer which corresponds to, $n = 1/p$, the fractional quantum number of the hydrogen-type molecule. Using Eqs. (B.246) and (B.248), the rotational energy absorbed by a hydrogen-type molecule with the transition from the state with the rotational quantum number J to one with the rotational quantum number $J + 1$ is

$$\Delta E = E_{J+1} - E_J = \frac{p^2\hbar^2}{m_p a_0^2}[J+1]$$

$$= p^2[J+1]2.37 \times 10^{-21} J. \tag{B.249}$$

The energy can be expressed in terms of wavelength in angstroms (Å) using the Planck relationship, Eq. (2.65)

$$\lambda = 10^{10} \frac{hc}{\Delta E} = \frac{8.38 \times 10^5}{p^2[J+1]}. \tag{B.250}$$

Vibration increases the internuclear distance, r of Eq. (B.241), which decreases the rotational energy. The rotational wavelength including vibration given in Section B.2.3 (Eq. (B.163)) is

$$\lambda = \frac{8.43 \times 10^5}{p^2[J+1]}. \tag{B.251}$$

The calculated wavelength for the $J = 0 \rightarrow 1$ transition of the hydrogen molecule $H_2(n = 1)$ including vibration is 8.43×10^5 Å. The experimental value is 8.43×10^5 Å [44].

B.7.2. Diatomic molecular rotation of hydrogen-type molecular ions

The moment of inertia of hydrogen-type molecular ions is given by substitution of the reduced mass, Eq. (B.247), for μ of Eq. (B.241) and substitution of the internuclear distance, two times Eq. (B.67), for r of Eq. (B.241)

$$I = m_p \frac{2a_0^2}{p^2}, \tag{B.252}$$

where p is an integer which corresponds to, $n = 1/p$, the fractional quantum number of the hydrogen-type molecular ion. Using Eqs. (B.246) and (B.242), the rotational energy absorbed by a hydrogen-type molecular ion with the transition from the state with the rotational quantum number J to one with the rotational quantum number $J + 1$ is

$$\Delta E = E_{J+1} - E_J = \frac{p^2\hbar^2}{m_p 2a_0^2}[J+1]$$

$$= p^2[J+1]1.89 \times 10^{-21} J. \tag{B.253}$$

The energy can be expressed in terms of wavelength in microns (μm) using the Planck relationship, Eq. (2.65).

$$\lambda = 10^6 \frac{hc}{\Delta E}\ \mu\text{m} = \frac{168}{p^2[J+1]}\ \mu\text{m}. \tag{B.254}$$

Vibration increases the internuclear distance, r of Eq. (B.241), which decreases the rotational energy. The rotational wavelength including vibration given in Section B.1.3 (Eq. (B.124)) is

$$\lambda = \frac{169}{p^2[J+1]}\ \mu\text{m}. \tag{B.255}$$

The calculated wavelength for the $J = 0 \rightarrow 1$ transition of the hydrogen molecular ion $H_2[2c' = 2a_0]$ including vibration is 169 μm. The experimental value is 169 μm [43].

References

[1] Mills R. The grand unified theory of classical quantum mechanics. January 2000 ed. Cranbury, New Jersey: BlackLight Power, Inc. Distributed by Amazon.com; posted at www.blacklightpower.com.

[2] Mills R. The grand unified theory of classical quantum mechanics, Global Foundation, Inc. Orbis Scientiae entitled The role of attractive and repulsive gravitational forces in cosmic acceleration of particles the origin of the cosmic gamma ray bursts. 29th Conference on High Energy Physics and Cosmology Since 1964. Dr. Behram N. Kursunoglu, Chairman, December 14–17, 2000, Lago Mar Resort, Fort Lauderdale, FL.

[3] Mills R. The grand unified theory of classical quantum mechanics, Global Foundation, Inc. Orbis Scientiae entitled The role of attractive and repulsive gravitational forces in cosmic acceleration of particles the origin of the cosmic gamma ray bursts. 29th Conference on High Energy Physics and Cosmology Since 1964. Dr. Behram N. Kursunoglu, Chairman, December 14–17, 2000, Lago Mar Resort, Fort Lauderdale, FL, New York: Kluwer Academic/Plenum Publishers, p. 243–258.

[4] Mills R. The grand unified theory of classical quantum mechanics. Int J Hydrogen Energy, in press.

[5] Mills R. The hydrogen atom revisited. Int J Hydrogen Energy 2000;25(12):1171–83.

[6] Mills R. The nature of free electrons in superfluid helium — a test of quantum mechanics and a basis to review its foundations and make a comparison to classical theory. Int J Hydrogen Energy 2001;26(10):1059–96.

[7] Mills R, Ray P. Spectral emission of fractional quantum energy levels of atomic hydrogen from a helium–hydrogen plasma and the implications for dark matter. Int J Hydrogen Energy, in press.

[8] Mills R, Ray P. Spectroscopic identification of a novel catalytic reaction of potassium and atomic hydrogen and the hydride ion product. Int J Hydrogen Energy, in press.
[9] Mills R. Spectroscopic identification of a novel catalytic reaction of atomic hydrogen and the hydride ion product. Int J Hydrogen Energy 2001;26(10):1041–58.
[10] Mills RL, Voigt A, Ray P, Nansteel M, Dhandapani B. Measurement of hydrogen balmer line broadening and thermal power balances of noble gas-hydrogen discharge plasmas. Int J Hydrogen Energy, submitted.
[11] Mills R, Greenig N, Hicks S. Optically measured power balances of anomalous discharges of mixtures of argon, hydrogen, and potassium, rubidium, cesium, or strontium vapor. Int J Hydrogen Energy, submitted.
[12] Mills R, Nansteel M. Argon–hydrogen–strontium plasma light source. IEEE Trans Plasma Sci., submitted.
[13] Mills R, Nansteel M, Lu Y. Excessively bright hydrogen–strontium plasma light source due to energy resonance of strontium with hydrogen. Europ J Phys D, submitted.
[14] Mills R, Dong J, Lu Y. Observation of extreme ultraviolet hydrogen emission from incandescently heated hydrogen gas with certain catalysts. Int J Hydrogen Energy 2000; 25:919–43.
[15] Mills R. Observation of extreme ultraviolet emission from hydrogen–KI plasmas produced by a hollow cathode discharge. Int J Hydrogen Energy 2001;26(6):579–92.
[16] Mills R. Temporal behavior of light-emission in the visible spectral range from a Ti–K_2CO_3-H-Cell. Int J Hydrogen Energy 2001;26(4):327–32.
[17] Mills R, Onuma T, Lu Y. Formation of a hydrogen plasma from an incandescently heated hydrogen-catalyst gas mixture with an anomalous afterglow duration. Int J Hydrogen Energy 2001;26(7):749–62.
[18] Mills R, Nansteel M, Lu Y. Observation of extreme ultraviolet hydrogen emission from incandescently heated hydrogen gas with strontium that produced an anomalous optically measured power balance. Int J Hydrogen Energy 2001;26(4):309–26.
[19] Mills R, Dhandapani B, Nansteel M, He J, Voigt A. Identification of compounds containing novel hydride ions by nuclear magnetic resonance spectroscopy. Int J Hydrogen Energy 2001;26(9):965–79.
[20] Mills R, Dhandapani B, Greenig N, He J. Synthesis and characterization of potassium iodo hydride. Int J Hydrogen Energy 2000;25(12):1185–203.
[21] Mills R. Novel inorganic hydride. Int J Hydrogen Energy 2000;25:669–83.
[22] Mills R. Novel hydrogen compounds from a potassium carbonate electrolytic cell. Fusion Technol 2000;37(2): 157–82.
[23] Mills R, Dhandapani B, Nansteel M, He J, Shannon T, Echezuria A. Synthesis and characterization of novel hydride compounds. Int J Hydrogen Energy 2001;26(4):pp. 339–67.
[24] Mills R. Highly stable novel inorganic hydrides. J Mater Res, submitted.
[25] Mills R, Good W, Voigt A, Jinquan Dong, Minimum heat of formation of potassium iodo hydride. Int J Hydrogen Energy, in press.
[26] Mills R. BlackLight power technology — a new clean hydrogen energy source with the potential for direct conversion to electricity. Proceedings of the National Hydrogen Association, 12th Annual US Hydrogen Meeting and Exposition, Hydrogen: The Common Thread, The Washington Hilton and Towers, Washington DC, March 6–8, 2001, p. 671–97.
[27] Mills R. BlackLight power technology — a new clean energy source with the potential for direct conversion to electricity. Global Foundation International Conference on Global Warming and Energy Policy, Dr. Behram N. Kursunoglu, Chairman, Fort Lauderdale, FL, November 26–28, 2000, New York: Kluwer Academic/Plenum Publishers, p. 1059–96.
[28] Sidgwick NV. The chemical elements and their compounds, Vol. I. Oxford: Clarendon Press, 1950. p. 17.
[29] Lamb MD. Luminescence spectroscopy. London: Academic Press, 1978. p. 68.
[30] Thompson BJ. Handbook of nonlinear optics. New York: Marcel Dekker, Inc., 1996. p. 497–548.
[31] Shen YR. The principles of nonlinear optics. New York: Wiley, 1984. p. 203–10.
[32] de Beauvoir B, Nez F, Julien L, Cagnac B, Biraben F, Touahri D, Hilico L, Acef O, Clairon A, Zondy JJ. Phys Rev Lett 1997;78(3):440–3.
[33] Livingston W, Wallace L. An atlas of the solar spectrum in the infrared from 1850 to 9000 cm^{-1} (1.1–5.4 μm) with identifications of the main solar features. Published by the National Optical Astronomy Observatories, December 18, 1990.
[34] Delbouille L, Roland G, Brault J, Testerman L. Photometric atlas of the solar spectrum from 1850 to 10,000 cm^{-1}, Kitt Peak National Observatory, Tucson, AZ.
[35] Migeotte M, Neven L, Swensson J. The solar spectrum from 2.8 to 23.7 microns, Part II. Measurements and identifications with W.S. Benedict, Comments on the spectra of telluric H_2O and CO_2 as observed in the solar spectrum. 2.8–23.7 microns, Institut D'Astrophysique De L'Universite' De Liege Observatoire Royal De Belgique, Technical Final Report-Phase A (Part II) Under Contract AF 61 (514)–432.
[36] Cohen L. An atlas of solar spectra between 1175 and 1950 Angstroms recorded on skylab with the NRL's Apollo telescope mount experiment, Laboratory for Astronomy and Solar Physics, Goddard Space Flight Center, NASA Reference Publication 1069, March, 1981.
[37] Haus HA. On the radiation from point charges. Amer J Phys 1986;54:1126–9.
[38] Jahnke-Emde, Tables of functions. 2nd ed. Stuttgart: Teubner, 1933.
[39] Fowles GR. Analytical mechanics. 3rd ed. New York: Holt, Rinehart, and Winston, 1977. p. 154–5.
[40] Fowles GR. Analytical Mechanics. 3rd ed. New York: Holt, Rinehart, and Winston, 1977. p. 57–66.
[41] Mizushima M. Quantum mechanics of atomic spectra and atomic structure. New York: W.A. Benjamin, Inc., 1970. p. 17.
[42] Atkins PW. Physical chemistry. 2nd ed. San Francisco: W.H. Freeman, 1982. p. 589.
[43] Nellis WJ. Making metallic hydrogen. Sci Amer 2000; p. 84–90.
[44] Roncin JY, Launay F, Larzilliere M. High resolution emission spectrum of H_2 between 78 and 118 nm. Can J Phys 1984;62:1686–705.